Separation and Purification Technology 263 (2021) 118358

Contents lists available at ScienceDirect

Separation and Purification Technology

journal homepage: www.elsevier.com/locate/seppur

Biopurification of monoclonal antibody (mAb) through crystallisation

Wenqian Chen [a], Xiaoyu Li [a], Mingxia Guo [a], Frederik J. Link [a], Siti S. Ramli [b], Jinbo Ouyang [c], Ian Rosbottom [a], Jerry Y.Y. Heng [a,d,*]

[a] Department of Chemical Engineering, Imperial College London, London SW7 2AZ, UK
[b] Department of Food Technology, Faculty of Applied Sciences, University Technology MARA (UiTM), Shah Alam, Selangor, Malaysia
[c] State Key Laboratory for Nuclear Resources and Environment, East China University of Technology, Nanchang 330013, PR China
[d] Institute for Molecular Science and Engineering, Imperial College London, London SW7 2AZ, UK

ARTICLE INFO

Keywords:
Biopurification
Protein crystallisation
Monoclonal antibody
Phase behaviour
Scale-up

ABSTRACT

Therapeutics based on monoclonal antibody (mAb) represent the most advanced biopharmaceuticals, being able to treat a wide range of challenging diseases such as cancers and arthritis. As the scale of mAb production steadily increases with the demand for mAb-based therapeutics, the downstream biopurification continues to experience significant bottleneck due to the throughput limited nature of the current purification technology. Over the last decades, significant advances have been made in protein (and especially mAb) crystallisation as an alternative biopurification technology that offers high product stability and purity as well as scalability. This review starts with the discussion of general physicochemical properties of mAb before moving on to the in-depth discussion of the distinct phase behaviour of mAb in comparison with conventional globular proteins such as lysozyme. The final part of this review presents a summary of successful demonstrations of crystallisation scale-ups of mAb and discusses the critical factors (i.e. mixing and temperature control) to be considered.

1. Introduction

Monoclonal antibody (mAb) is a type of high value protein in the pharmaceutical industry. According to the International Union of Pure and Applied Chemistry (IUPAC) Recommendation 1992, mAbs are defined as "single species of immunoglobulin molecules produced by culturing a single clone of a hybridoma cell ….. (that) recognizes only one chemical structure, i.e. they are directed against a single epitope of the antigenic substance used to raise the antibody [1]." The high specificity of mAb towards the biological target is achieved with the antigen binding site (Fig. 1) that binds selectively to the antigen present on the biological target. Such high specificity enables the treatment of difficult diseases with mAb-based therapeutics, which cause significantly less side-effects as compared with their small molecule counterparts [2,3].

The manufacturing of mAb can be divided into upstream and downstream (Fig. 2), where upstream refers to the biological synthesis of mAb and the downstream refers to the purification and formulation of mAb. In the upstream (Fig. 2 left), mAb is generated with recombinant technology, where the light and heavy chain antibody genes are cloned and expressed in mammalian cells, such as Chinese Hamster Ovary (CHO), NS0 and Sp2/0 cells [5,6]. CHO cell is the most popular choice in upstream as it has advantages such as fast growth, high expression and high adaptability in chemically defined media. With nutrients added periodically to the cells in the bioreactor, a typical batch production process runs for 1 – 2 weeks to produce mAb at 1–5 g/L titer, but higher titers (i.e. 10–13 g/L) have been reported [6].

The industrial downstream purification of mAb (Fig. 2 right) starts with the centrifugation step for cell removal, which is followed by a series of chromatographic steps for the removal of key impurities including host cell proteins, DNA and virus. In the final product, the concentration of host cell proteins must be reduced to parts per million (ppm), whereas the concentration of DNA must be reduced to parts per billion (ppb) and the virus content must be reduced to less than one virus particle per million doses [7]. Traditionally, the most important purification step is affinity chromatography (i.e. "Protein A Chromatography" in Fig. 2 right), where the clarified cell mixture containing mAb and other impurities passes through a column of resin that binds selectively with mAb [8]. The resin is functionalised with protein-A, which is a single chain protein with a molecular weight of 42 kDa and 5 domains that bind with the Fc of IgG [4]. In order to recover the mAb, an acidic buffer typically at pH 2.5–4.0 is passed through the column of resin to weaken the hydrophobic interaction between the Fc of IgG and protein-

* Corresponding author.
E-mail address: jerry.heng@imperial.ac.uk (J.Y.Y. Heng).

https://doi.org/10.1016/j.seppur.2021.118358
Received 8 January 2021; Accepted 16 January 2021
Available online 20 January 2021

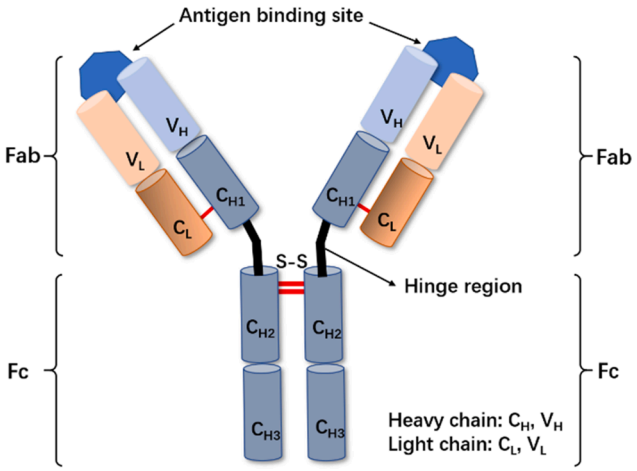

Fig. 1. General structure of IgG (the most common type of mAb) (adapted from [4]).

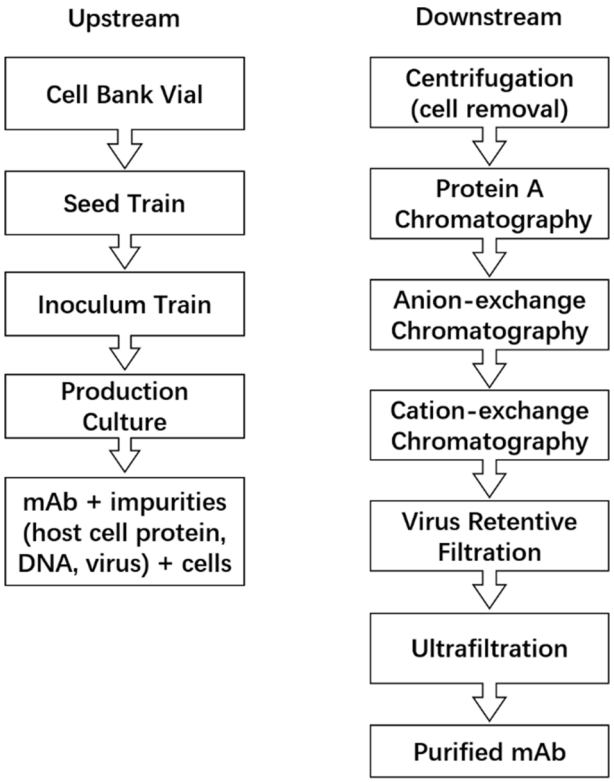

Fig. 2. General manufacturing process of mAb (left: upstream; right: downstream) (adapted from [6]).

A to recover the IgG in the solution form [8]. The affinity chromatography step is followed by several polishing steps where other types of chromatography such as ion exchange and hydrophobic interaction chromatographies are used to remove the remaining impurities.

Since the first approval of mAb-based therapeutic in 1986, the sales of mAb-based therapeutics have grown steadily over the past three decades (e.g. sales increased from approximately $75 billion in 2013 to $123 billion in 2017) [5,9]. In 2017, the five top-selling mAb-based therapeutics generated a total sales revenue of $50.2 billion with each achieving more than $7 billion (Table 1). mAb-based therapeutics have become the most important biologics in the pharmaceutical industry, accounting for more than half of the total sales of biologics between 2011 and 2018 [5].

Table 1
Five top-selling mAb-based therapeutics in 2017 [2,5].

Name	Antibody format	Brand name	Approval year	Sales revenue in 2017
Adalimumab	Human IgG1	Humira	2002	$18.9 billion
Etanercept	Fc fusion protein	Enbrel	1998	$8.3 billion
Rituximab	Chimeric IgG1	Rituxan	1997	$7.8 billion
Infliximab	Chimeric IgG1	Remicade	1998	$7.8 billion
Trastuzumab	Humanised IgG1	Herceptin	1998	$7.4 billion

The high efficacy of mAb-based therapeutics comes with high sales price, which creates tremendous financial burdens to the patients. For example, two of the top-selling mAb-based therapeutics, Rituxan and Enbrel, have a sales price of $4000 per gram and a patient requires several grams per treatment [6]. As the demand of mAb-based therapeutics continue to grow, the current high sales price creates a market for biosimilars, which are "highly similar replicate products of a therapeutic antibody that has already received marketing approval" [3] and have significantly lower sales price compared to the original product. Since 2006, 27 mAb-based biosimilars have been approved and all of them are replicates of the six top-selling mAb-based therapeutics in 2017 [5].

The rise of biosimilars means the production of mAb-based therapeutics will increase in scale to provide more affordable mAb-based therapeutics for patients. In order to benefit from the economy of scale, pharmaceutical companies will require more cost-effective manufacturing technologies of mAb, especially for replacing the affinity chromatography step that typically accounts for more than half of the downstream purification cost due to the high cost of protein-A resin [6,10,11]. "Anything but conventional chromatography" is a concerted effort in the academia and industry to develop alternative biopurification technologies including crystallisation [12–14], precipitation [15], filtration [16–18] and extraction [19–23] to achieve the same high product purity as protein-A chromatography, while overcoming the throughput limited nature of chromatography and avoiding the use of expensive consumables (i.e. resin) [7,24,25].

Among the emerging technologies, crystallisation is advantageous in terms of scalability, product purity and stability as demonstrated in the manufacturing of small molecule therapeutics [26], but also the most technically challenging due to the complex and flexible nature of protein in general [27,28]. Although protein crystallisation is difficult even at small scale, significant advancement for protein crystallisation as a scalable purification technology has been made over the past few decades in terms of the fundamental understanding of the phase behaviour of protein, the development of materials that promote crystallisation (i.e. heterogeneous nucleants) and process development of protein crystallisation [27,28].

This review focuses on the crystallisation of mAb based on the fundamental understanding of the phase behaviour and successful case studies for the scale-up of mAb crystallisation. The article starts with the discussion of the general properties of mAb as the background information before moving on to the in-depth discussions of the phase behaviour (especially crystallisation) of mAb under different external factors such as temperature and additive concentration and several successful examples of mAb crystallisation scale-ups from the engineering perspective.

2. General information of mAb

Most of the mAbs belong to immunoglobulin (Ig), which is defined as "a protein of the globulin-type found in serum or other body fluids that possesses antibody activity" [1]. Ig consists of two light and two heavy polypeptide chains linked by disulphide bonds. Based on the antigenic

and structural differences in the heavy chains, human Ig can be further divided into five general classes (A, D, E, G and M) [29], among which IgG provides most of the antibody-based immunity. Therefore, the discussion of mAb in this article mainly refers to IgG (Fig. 1).

Generally, IgG has a molecular weight of ~150 kDa, with each light chain and heavy chain accounting for ~25 kDa and ~50 kDa respectively. IgG has a Y-shape structure that consists of the antigen-binding and crystallisable fragments (Fab and Fc) (Fig. 1) [4]. The antigen-binding region locates at the top of the Fab and has the variable heavy (V_H) and variable light (V_L) segments. On the other hand, the Fc consists of three constant heavy segments (C_{H1}, C_{H2}, and C_{H3}) and is responsible for mediating immunal responses.

Since Kohler and Milstein reported an efficient production method for mAb in 1975 [30], the design of therapeutic mAbs has evolved to meet the medical needs [2]. The first generation of mAb (Fig. 3) failed to achieve the therapeutic purpose as they were based on murine molecules and caused significant rejection by the human body. As the antigen-binding region of mAb only accounts for a small section of the molecule, the amino acid sequence of mAb has been gradually replaced with the human version to make the second generation of mAb (Fig. 3) in order to reduce the rejection by human body while maintaining the capability of specific binding.

The second generation of mAb includes chimeric, humanised and fully human mAb in ascending order of similarity to human mAb (Fig. 3). A chimeric mAb has 70% human amino acid sequence with a fully human Fc, whereas a humanised mAb has 85 – 90% human amino acid sequence [2]. As the name suggests, fully human mAb has 100% human amino acid sequence and causes the least immunogenic reactions in human body. Four out of the five top-selling mAb-based therapeutics (Table 1) belong to the second generation of mAb. As mAb technology continues to improve, the third generation of mAb (e.g. antibody fragments, Fc fusion proteins, bispecific antibodies and intrabodies) has been developed to offer enhanced therapeutic performances. One of the five top-selling mAb-based therapeutics, etanercept, is a Fc fusion protein and belongs to this class of mAb (Table 1).

3. Protein-protein interaction and phase behaviour

Protein purification technologies such as crystallisation, precipitation and extraction are based on the phase behaviour of the target protein, which is the macroscopic manifestation of protein–protein interaction at the molecular level [31]. Electrostatic forces, van der Waal forces, hydrophobic forces, volume exclusion effect by polymer molecules, hydration layer and specific ion effects all play important roles in protein–protein interaction [32]. With respect to the target protein, these forces are dependent on both internal factor (i.e. the amino acid sequence of protein) and external factors (i.e. temperature, pH, types of solvent, types and concentration of additives). The amino acid sequence decides the physicochemical properties of the protein, including size, isoelectric point (pI) and 3D structure (e.g. shape and location of hydrophobic patches on the surface). Based on these physicochemical properties, external factors can be adjusted within a relatively narrow range to achieve the desirable protein–protein interaction, while maintaining the stability of the protein (i.e. protein is correctly folded and has its intended bioactivity) [27].

Compared to small molecules, proteins are highly complex due to their anisotropy in terms of shape and charge distribution. Efforts have been made to quantify protein–protein interaction by the osmotic second virial coefficient (B_{22}) and the viscosity & viscoelasticity of the protein/additive mixture (Fig. 4 (left)). B_{22} can be experimentally determined with static light scattering [33–35] and self-interaction chromatography [36], where the first method is suitable for dilute protein/additive mixtures to avoid the formation of oligomers and the second method is suitable for dealing with higher concentrations. B_{22} is used to calculate the osmotic pressure under non-ideal conditions (Eq. (1a)), where the magnitude of B_{22} is proportional to the extent of deviation from ideality (Eq. (1b)) [36]. Negative B_{22} means that the protein molecules are attractive towards one another and highly negative B_{22} means that the protein molecules tend to precipitate. Conversely, positive B_{22} means that the protein molecules repel one another and the protein solution is stable and remains clear.

Previous studies have shown that the determination of B_{22} is useful for identifying a general protein crystallisation region, which is often referred to as the "crystallisation slot" [37,38]. In this crystallisation region, B_{22} is slightly negative as protein molecules are weakly attractive to one another. Beyond this range of B_{22} in the negative direction, protein molecules are strongly attractive to one another and tend to precipitate instead of crystallising. As the suitable range of B_{22} for crystallisation is very narrow, high throughput screening of experimental conditions such as temperature, pH and additive concentrations is often conducted for identifying the suitable crystallisation conditions [39]. Similar to crystallisation, the occurrence of LLPS indicates the overall attractive nature of protein–protein interactions (i.e. negative B_{22}, but less than that for precipitation).

$$\Pi = k \times T \times \left(c + B_{22} \times c^2 + \cdots\right) \tag{1a}$$

$$\Pi \approx \Pi_{ideal} + k \times T \times B_{22} \begin{cases} B_{22} > 0 \rightarrow \Pi > \Pi_{ideal} (i.e. repulsive interaction) \\ B_{22} = 0 \rightarrow \Pi = \Pi_{ideal} (i.e. neutral interaction) \\ B_{22} < 0 \rightarrow \Pi < \Pi_{ideal} (i.e. attractive interaction) \end{cases} \tag{1b}$$

where Π is osmotic pressure, k is Boltzmann's constant, T is temperature, c is protein concentration and B_{22} is osmotic second virial coefficient which is determined experimentally.

In the case of highly concentrated protein/additive mixture, viscosity and viscoelasticity are more suitable for the study of protein–protein interaction as previous studies have shown that protein–protein interaction at high concentration is the result of multiple forces such as van der Waal force, electrostatic force and volume exclusion effect, and the net force is highly consistent with the viscosity and viscoelasticity of

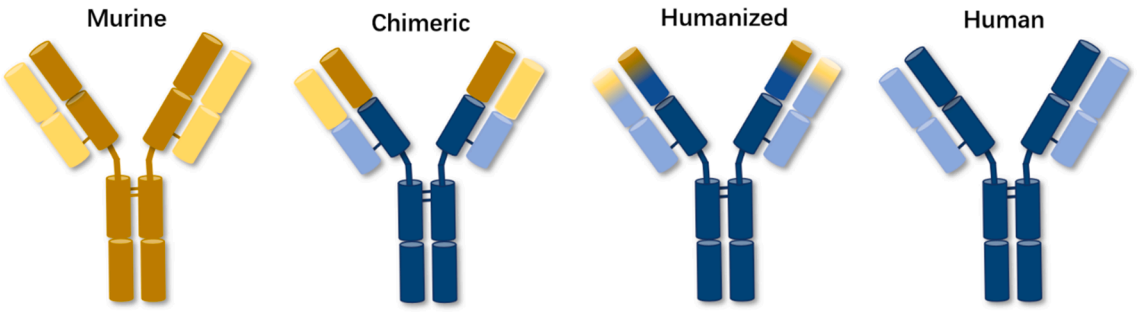

Fig. 3. mAb development: first generation = murine; second generation = chimeric, humanised and fully human where yellow regions are non-human amino acid sequences and blue regions are human amino acid sequences (adapted from [2]).

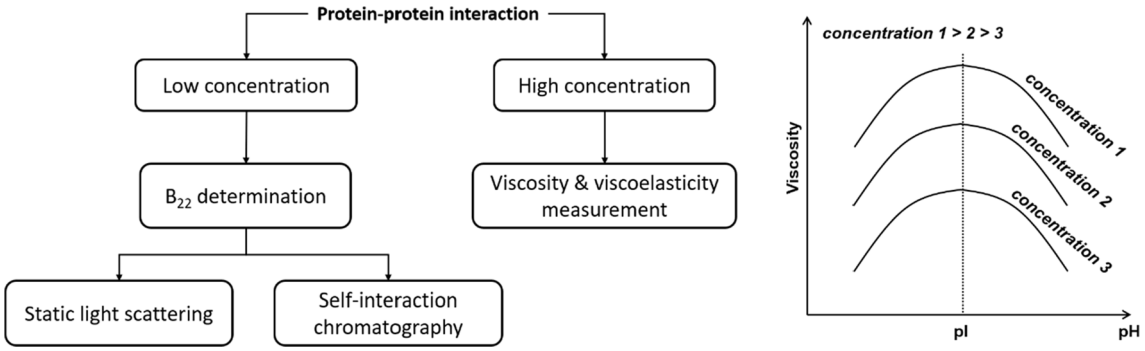

Fig. 4. (left) Strategy for experimentally determining protein–protein interaction and (right) protein viscosity over a range of pH at protein high concentration (based on the results of [40]).

protein solutions [32,40,41]. For instance, a case study of bovine serum albumin (BSA) showed that the protein–protein interaction was the strongest at pH = pI, where the protein molecules were neutral, electrostatic repulsions were the minimal and strong short-range attractive interactions became dominant. This was reflected in the viscosity measurement, where the viscosity was the highest at pH = pI and decreased with protein concentration at high protein concentration range (i.e. 40 – 300 mg/mL) (Fig. 4 (right)) [40]. As pH moves away from pI, the protein–protein interaction decreases as protein molecules have stronger electrostatic repulsions. The viscosity of protein solution decreases correspondingly. On another hand, the protein–protein interaction decreases with protein concentration and this is also reflected by the viscosity of protein solution (Fig. 4 (right)).

3a. General phase bahaviour

Table 2 summarises the existing studies on the phase behaviour of mAbs, which are mostly intact IgG1, IgG2 and IgG4. Although their molecular weights (MWs) are relatively similar (144 – 151 kDa), their pIs vary widely (4.6 – 9.2) as slight variations of the amino acid sequence in the Fab region can cause significant changes in the pI [42]. A wide range of pH, temperature and additives were tested in these studies, enabling the construction of a general phase diagram (Fig. 5), where solubility is defined as the overall mAb fraction in the dissolved state (i.e. clear mAb solution) at equilibrium with condensed phases (i.e. precipitate, crystal, dense droplet/network). In general, higher temperature (up to 60 °C as proteins start to unfold at approximately 70 °C [43]) can disrupt the protein–protein interaction (i.e. increasing B_{22} in the positive direction) and favour the solution state of protein molecules. As a result, mAb solubility increases with temperature in general (Fig. 5). A supersaturated protein solution (i.e. mAb fraction > solubility) can be created by adjusting the external conditions such as reducing temperature (i.e. moving vertically down in Fig. 5) to promote phase separation [44].

Based on the literature (Table 2), mAb in general often undergoes liquid–liquid phase separation (LLPS) together with or before the appearance of crystals [35,46,47]. This is represented as regions C and D in Fig. 5, where the binodal curve provides information about the mAb fraction in the light and heavy phases at a fixed temperature, similar to the spinodal curve. In region C (i.e. between the binodal curve and spinodal curve), binodal demixing occurs (i.e. droplets of protein heavy phase appear after an induction period) [48,49]. In region D (i.e. within the spinodal curve), spinodal decomposition occurs (i.e. networks of protein heavy phase appear instantly). As demonstrated in a study [50], the enrichment of mAb in the heavy phase could result in orders of magnitude difference between the concentrations in the heavy and light phases. By dialysing a protein solution with 8 – 65 mg/mL IgG1 against a dilute buffer (5 mM sodium phosphate, 10 mM sodium chloride, 5% sucrose, pH = 5.5) at 5 °C, LLPS was induced. The IgG1 concentrations in the heavy and light phases were 215 mg/mL and 2 mg/mL respectively regardless of the IgG1 concentration before LLPS. Another study also confirmed the huge difference of mAb concentration in heavy and light phases [51].

The most important factor for the general phase behaviour of mAb (Fig. 5) is the size of mAb molecule relative to the effective range of protein–protein interactions, including hydration, hydrophobic, van der Waals and electrostatic interactions as well as ionic bridges [48]. The effective range of these interactions vary from a few Angstroms to approximately one nanometer [52–60], which is significantly shorter than the hydrodynamic diameter of mAb (~10 nm) [35,50,61]. As a result, mAb molecules resemble colloidal particles with short range interactions in terms of phase behaviour as demonstrated by simulation studies [38,45,62–66].

Although mAb shares similar phase behaviour (Fig. 5) with other globular proteins, there are subtle differences that must be considered for the successful crystallisation of mAb. The origins of differences are the relatively larger size and high flexibility of mAb. Firstly, as proteins consist of amino acids with different side chains that have different physicochemical properties, larger proteins in general have higher degree of anisotropy (e.g. the distribution of surface charges and hydrophobic patches). Due to the large size of mAb (molecular weight ~ 150 kDa vs 15 kDa (lysozyme) and 68 kDa (bovine serum albumin) [67,68]), mAb in general has high degree of anisotropy that hinders crystallisation, as it is more difficult to arrange these molecules in an orderly structure [34]. For example, the high degree of anisotropy can be demonstrated by the vastly different physicochemical properties of the Fab and Fc of mAb [43]. Secondly, compared with other globular proteins such as lysozyme (hydrodynamic diameter ~ 4 nm) [67], mAb is relatively larger in size (hydrodynamic diameter ~ 10 nm) [35,50,61]. As a result, the protein–protein interactions mentioned above are even more short-range for mAb than other globular proteins and LLPS tends to occur at substantially lower protein concentration for mAb (e.g. 87 mg/mL for an IgG2 vs 230 mg/mL for lysozyme) [69,70]. Thirdly, mAb has a high degree of flexibility due to the hinge region that connects Fab and Fc (Fig. 1). It was shown previously that deleting the hinge could reduce the flexibility of mAb and increase the success rate of crystallisation [71,72]. Although this approach is useful in the study of 3D structure of mAb, it is not feasible in the crystallisation of mAb for purification purposes, where the structure of mAb must remain intact.

Although crystallising mAb is more challenging than other globular proteins, the tendency of mAb to undergo LLPS can be a useful characteristic for improving the success rate of crystallisation as crystallisation of mAb often occurred together with LLPS in existing literature (Table 2). In Fig. 5 (both left and right), region B refers to the crystallisation region where no LLPS occurs and nucleation follows the classical nucleation theory [45]. In region C and D, LLPS occurs and there is a significant enrichment of mAb in the heavy phase (also referred to as the “protein-rich phase” and “dense phase” during LLPS [50,51]. It was

Table 2
Summary of phase behaviour studies of mAb.

Types of mAb*	Experimental conditions					Observed phase changes	Ref.
	Buffer type	pH	Temperature	Protein concentration	Additives concentration		
mAbMW = 145 kDa	• 100 mM HEPES	6.8 – 8.2	20 °C	< 60 mg/mL	• Na_2SO_4 (<1.51 M) • $(NH_4)_2SO_4$ (<1.5 M) • Li_2SO_4 (<1.5 M) • $MgSO_4$ • $ZnSO_4$ • PEG 400 (<12% w/v)	• Liquid-liquid phase separation promoted by PEG400 and Na_2SO_4, Li_2SO_4 and $(NH_4)_2SO_4$. • Crystallisation occurred after or simultaneously with liquid–liquid phase separation.	[35,46]
IgG4 (x1) IgG4 + antigen (x1) Fab (x4)	• 100 mM HEPES	7.5	4 – 18 °C	< 9 mg/mL	• Li_2SO_4 (<2 M) • PEG 400 (<2.5%) • PEG 550 MME • PEG 600 • PEG 1000 (<2.5%) • PEG 2000 • PEG 3350 (<10%) • PEG 8000 (<2.5%) • PEG 20,000 (<2.5%) • Jeffamine ED 90 • Jeffamine ED 600 • Jeffamine ED 2,000 (<2.5%) • Jeffamine ED 4,000 (<2.5%) • MPD (<2.5%) • Polyvinylpyrolidone 15 • Polyacrylic Acid 5100 • Ultra low Visc. Carboxymethylecellulose • Medium Visc. Carboxymethylecellulose • High Visc. Carboxymethylecellulose • Polyvinyl alcohol 15,000 • Polypropylene glycol P400 • Polyacrylic Acid 2100	• No crystal formation without PEG or Jeffamine. • Co-existence of crystal and liquid–liquid phase separation observed. • Ideal crystallisation conditions identified (i.e. Li_2SO_4 (1 – 2 M), PEG 3350 (0.1 – 0.3%) or Jeffamine ED 2000 & 4000 (0.1 – 0.3%) • Jeffamine ED 2000 was the most promising additive	[47]
mAb(type unspecified) • MW = ~ 144 kDa • pI = ~ 8	• 10 mM sodium phosphate	4.2 – 9.5	30 °C	<100 mg/mL	• $(NH_4)_2SO_4$ (<1.5 M) • NaCl (<4.5 M) • PEG 400 (<25% v/v)	• Precipitation as salt and PEG 400 concentration increased.	[31]
mAb(type unspecified) • MW = ~ 144 kDa • pI = ~ 8 *same molecule as in the row above	• 10 mM sodium formate • 10 mM sodium acetate • 5 mM bis-tris	3–7	23 °C	< 70 mg/mL	• $(NH_4)_2SO_4$ (<1.4 M) • Li_2SO_4 (<1.4 M) • $MgSO_4$ (<1.6 M) • NaCl (<2.0 M) • PEG 3350 (<8 wt%)	• Liquid-liquid phase separation and then precipitation as sulphate salt concentration increased. • No phase change in NaCl. • Liquid-liquid phase separation and crystallisation in $(NH_4)SO_4$ and Li_2SO_4 at pH 5. • Liquid-liquid phase separation and then crystallisation in $(NH_4)SO_4$ as PEG 3350 concentration increased.	[36]
IgG1 (x4) • pI = 7.4 – 9.2 • MW = 145 – 150 kDa IgG2 (x16) • pI = 5.8 – 8.8 • MW = 144 – 151 kDa Fc-fusion protein (x2) • pI = 4.6 – 5.7 • MW = 76 – 102 kDa	• 700 mM sodium MES • 850 mM sodium citrate • 1 M sodium phosphate • 1 M Tris acetate • 2 M Tris chloride	5.5 – 9.0	22 °C	< 100 mg/mL	• Na_2SO_4 (1 M) • PEG 3350 (25% v/v)	• Liquid-liquid phase separation for IgG1 at high protein and salt concentrations. • Liquid-liquid phase separation and crystallisation in the presence of PEG 3350 for 7 out of 16 IgG_2. • Liquid-liquid phase separation in the presence of Na_2SO_4 for the remaining 9 of 16 IgG_2. • Liquid-liquid phase separation for Fc-fusion protein when pH approached pI. • Liquid-liquid phase separation and crystallisation in salting-in regions.	[104]
IgG1 (x3) IgG2 (x2)	• 50 mM citric acid • 50 mM sodium citrate • 50 mM MES • 50 mM bis-tris • 50 mM imidazole • 50 mM HEPES • 50 mM Tris	3.0 – 9.0	4 – 37 °C	< 5 mg/mL	• PEG 3350 (≤24%) • PEG 8000 • Detergents (x49)	• Crystallisation in the presence of PEG 3350 apparently more than PEG 8000. • Crystallisation in low PEG 3350 (4 – 12%). • Liquid-liquid phase separation observed frequently. • Liquid-liquid phase separation could turn into crystallisation. • Crystallisation enhanced by detergents.	[95]
IgG1	• 100 mM MES		−2 – 35 °C	≤ 20 mg/mL			[61]

(*continued on next page*)

Table 2 (*continued*)

Types of mAb*	Experimental conditions					Observed phase changes	Ref.
	Buffer type	pH	Temperature	Protein concentration	Additives concentration		
• pI = 4.7 (room temperature)	• 100 mM Glycine-HCl	6 – 7			• PEG 1000 (5 – 11% w/v (mg/mL)) • PEG 1500 (5 – 11% w/v (mg/mL)) • PEG 3350 (5 – 11% w/v (mg/mL)) • PEG 6000 (5 – 11% w/v (mg/mL))	• Liquid-liquid phase separation promoted by higher PEG concentration and molecular weight. • Crystal formation (co-existing with liquid–liquid phase separation) in PEG 1000.	
IgG1 (x2) • pI = 8.2 – 8.9 IgG4 (x1) • pI = 8.3 – 8.8	• 10.1 mM MES, 16.6 mM acetic acid,8.9 mM MOPSO,12.3 mM HEPPSO, • 14.4 mM CHES	5 – 9	room temperature	< 30 mg/mL	• $(NH_4)_2SO_4$ (<1.6 M) • Li_2SO_4 (<1.4 M) • Na_2SO_4 (<0.6 M) • NH_4Cl • NaCl (<2.6 M)	• No liquid–liquid phase separation observed. • Success rate of crystallisation increased when pH ~ pI. • Crystallisation and then precipitation occurred as salt concentration increased. • Gelation instead of crystallisation could occur before precipitation. • Needle-crystal formation at low Li_2SO_4 (0.5 M).	[94]
IgG1 (x4) IgG2 (x2) IgG4 (x1) IgG (unspecified) (x1)	• 10 mM sodium formate • 10 mM sodium acetate • 5 mM bis-tris	3 – 7	room temperature	< 70 mg/mL	• $(NH_4)_2SO_4$ (<1.2 M) • Li_2SO_4 (<1.0 M) • NaCl (<4 M) • PEG 3350 (<6%)	• Phases changes occurred in sulphate salts, while only one (out of eight) IgG had phase change in NaCl. • Liquid-liquid phase separation and crystallisation promoted by high salt and PEG concentrations.	[92]
IgG1 (x2) IgG4 (x1)	• 10.1 mM MES, 16.6 mM acetic acid,8.9 mM MOPSO,12.3 mM HEPPSO,14.4 mM CHES	5 – 9	room temperature	≤ 10 mg/mL	• PEG 400 (<20 m/V%) • PEG 1000 (<15 m/V%) • PEG 3350 (<12.5 m/V%) • PEG 8000 (<12.5 m/V%)	• Crystallisation and precipitation promoted by increasing molecular weight of PEG. • Crystal size dependent on molecular weight of PEG (1000 and 3350 promoted the formation of larger crystals compared to PEG 400 and 8000) and PEG concentrations. • Liquid-liquid phase separation promoted by larger PEG.	[33]
IgG1 (x2) IgG4 (x1)	• 10 mM MES	5 – 9	room temperature	< 10 mg/mL	• $(NH_4)_2SO_4$ (<1 M) • Li_2SO_4 (<1 M)	• Crystallisation more successful in $(NH_4)_2SO_4$.	[34]
IgG2 (x5)	• Phosphate buffered saline • 20 mM sodium acetate	5 – 7.4	−5 – 30 °C	< 2 mg/mL	• PEG 3350 (<21% w/w) • PEG 4600 (<11% w/w) • PEG 6000 (<11% w/w) • PEG 8000 (<11% w/w)	• Liquid-liquid phase separation occurred in the presence of PEG. • Liquid-liquid phase separation occurred at lower temperature as molecular weight of PEG increased.	[96]
IgG2 • pI = 7.2 • MW = ~ 148 kDa	• 22 mM potassium phosphate	5.3 – 7.1	−10 – 3 °C	< 90 mg/mL	• KF • KCl • KSCN	• Liquid-liquid phase separation at pH close to pI not affected by anion type of salt at low ionic strength. • Liquid-liquid phase separation at pH close to pI affected by anion type of salt at high ionic strength (following direct Hoffmeister series where F^- encouraged separation more than Cl^- and SCN^-). • Liquid-liquid phase separation at pH below pI affected by anion type of salt (following inverse Hoffmeister series where SCN^- encouraged separation more than Cl^- and F^-). • Crystal formation in buffer at pH near pI at high protein concentration (i.e. 90 mg/mL).	[69]
IgG1 • pI = 6.5	• 5 mM sodium phosphate	5 – 7	5 – 50 °C	< 165 mg/mL	• NaCl (<40 mM) • Polysorbate 80	• Liquid-liquid phase separation promoted by lowering the temperature (protein concentration in the heavy phase increased with lower temperature). • Liquid-liquid phase separation promoted by bringing pH close to pI.	[50]
IgG1 (x2) • pI = 8.9 – 9.0 IgG2 (x3) • pI = 6.8 – 8.8	• 20 mM sodium phosphate • 100 mM sodium acetate	3.5 – 6.8	4 – 80 °C	< 25 mg/mL	• NaCl (<1 M) • Caprylic acid • Heptanoic acid	• No aggregation up to 60 °C. • Temperature-induced aggregation behaviour was similar between Fab and intact IgG. • Aggregation occurred under rigorous agitation. • Aggregation promoted by low pH.	[43]

(*continued on next page*)

Table 2 (*continued*)

Types of mAb*	Experimental conditions					Observed phase changes	Ref.
	Buffer type	pH	Temperature	Protein concentration	Additives concentration		
						• Aggregation induced by fatty acids (i.e. caprylic acid & heptanoic acid). • Liquid-liquid phase separation occurred at low temperature (Fc had similar concentrations in heavy and light phase; Fab enriched in the heavy phase).	
IgG2	• 100 mM tris-HCl	7.4	−7 – 0 °C	< 100 mg/mL	• Human serum albumin	• Liquid-liquid phase separation occurred at low temperature. • Liquid-liquid phase separation unfavoured by human serum albumin (human serum albumin enriched in the heavy phase).	[51]
IgG1 (x8)	• Phosphate saline buffer	7.4	−10 – 35 °C	< 100 mg/mL	• PEG 3350	• Liquid-liquid phase separation promoted by PEG 3350. • Crystallisation observed after liquid–liquid phase separation.	[49]
IgG1 (x4) • pI = 7.5 – 9.0 IgG2 (x4) • pI = 7.2 – 8.8	• 20 – 500 mM sodium acetate • 20 mM phosphate	5.0 – 7.5	4 – 21 °C		• PEG 8000	• Liquid-liquid phase separation induced by high PEG 8000 concentration as pH moved away from pI (pH < pI).	[99]
IgG4	• 100 mM imidazol	7	room temperature		• Calcium acetate (0.2 M) • PEG 8000 (<10% w/v)	• Crystallisation directly from clarified cell culture.	[105]
mAb(unspecified) • MW = 145 kDa • pI = 8.3		6.5 – 9.0	5 – 20 °C	< 100 mg/mL	• NaCl • Citrate	• Liquid-liquid phase separation occurred at pH close to pI. • Liquid-liquid phase separation promoted by low temperature and salts (even at low ionic strength).	[106]

* Intact unless stated otherwise.

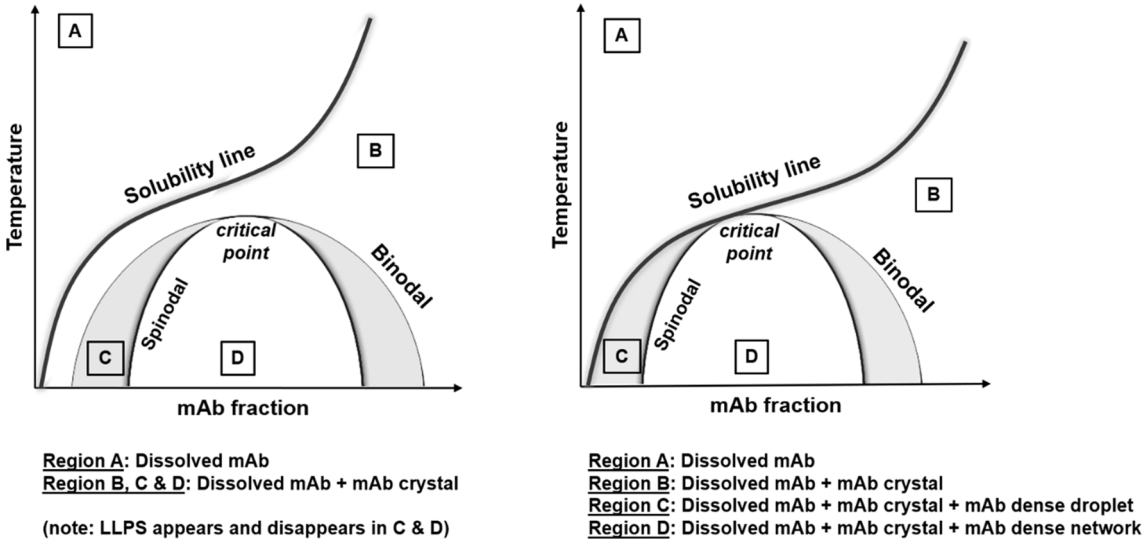

Fig. 5. General phase diagram of mAb with liquid–liquid phase separation (LLPS) (i.e. regions C & D) that is transient (left) and stable (right) (adapted from [34,45]).

demonstrated previously that for LLPS induced by salt and suitable temperature, there was no partitioning of salt in the light and heavy phases (i.e. the salt concentrations were the same in both phases) [66]. Therefore, the high concentration of mAb within the heavy phase (i.e. dense droplets) creates a significantly higher degree of supersaturation that enhances the nucleation. The nucleation follows the two-step mechanism with the formation of the dense droplets followed by the nucleation within the droplets [45,48,73]. It was shown previously that protein nucleation rate was the highest in conditions where the system transitioned from a clear solution to LLPS [74]. Interestingly, when a soluble polymer such as polyethylene glycol (PEG) is used, the droplet periphery has been observed as the first site of crystal appearance, indicating a different nucleation mechanism that requires more investigation efforts in the future [35,75].

3b. Effect of temperature on phase behaviour

From the perspective of thermodynamics, the change of Gibbs free energy (ΔG) must be negative for a phase change to occur. Under isothermal conditions, the change of Gibbs free energy is related to the change of enthalpy (ΔH) and change of entropy (ΔS) by Eq. (2). In the current context, the initial state refers to the solution state, where protein molecules are dissolved completely in a solvent system at a specific temperature under atmospheric pressure, and the final state refers to the

phase separated state, where the protein molecules in the dissolved form co-exist with protein molecules in the condensed forms (i.e. dense liquid droplet and/or precipitate and/or crystal) under the same temperature and pressure.

$$\Delta G = \Delta H - T \times \Delta S \quad (2)$$

In general, if only the protein molecules are considered, the transition from the solution state to phase separated state means $\Delta S < 0$ as the protein molecules are more closely arranged in space. This means the phase separation process must be sufficiently exothermic (i.e. $\Delta H < 0$) for the process to take place. In this case, the protein has an upper critical solution temperature (UCST) behaviour which means lowering temperature favours phase separation (Fig. 6 (left)). For protein crystallisation, lysozyme has a UCST behaviour in general and is easily crystallisable due to the highly negative $\Delta H_{\_crystallisation}$ over a broad range of conditions (e.g. $\Delta H_{\_crystallisation}$ = -100 kJ/mol in 0.2 – 0.6 M NaCl at 4.2 < pH < 4.7 and 15 – 30 °C [76]).

For proteins whose $\Delta H_{\_crystallisation}$ is close to zero (e.g. apoferritin [79] and lumazine synthase [80]) or even positive (e.g. haemoglobin [81]), the overall change in entropy during crystallisation (i.e. $\Delta S_{\_crystallisation}$) must be positive, which is possible with the release of water molecules originally bound to the additive and protein molecules as the result of strong binding of additive molecules to protein molecules [82]. In this case, the protein has lower critical solution temperature (LCST) behaviour which means raising temperature favours phase separation (Fig. 6 (right)).

Based on the literature (Table 2), mAb in general has a UCST behaviour (Fig. 6 (left)). As a plasma protein, mAb is usually highly soluble at physiological conditions and only undergoes LLPS below 0 °C [49]. Increasing the temperature reduces the extent of partitioning and hence the mAb concentration difference between the heavy and light phases until the critical point, above which LLPS disappears and a clear solution is obtained (Fig. 6 (left)). In a previous study [50], increasing the temperature caused the IgG1 concentrations in the heavy and light phases changed from 215 mg/mL and 2 mg/mL respectively at 5 °C to 136 mg/mL and 11 mg/mL respectively at 25 °C, reducing the IgG1 concentration difference from 100 folds to slightly more than 10 folds. Such UCST behaviour has been observed for other globular proteins such as lysozyme [83] and a partially miscible mixture [84]. In stark contrast, nonionic surfactant has an LCST behaviour (i.e. LLPS is enhanced by increasing temperature) (Fig. 6 (right))[50,61,69,77,78,85]. As LLPS tends to promote mAb crystallisation, the UCST behaviour of mAb in general means reducing temperature is favourable for mAb crystallisation.

3c. Effect of pH and salts on phase behaviour

Similar with other globular proteins, pH and salts have significant effects on the phase behaviour of mAb. Based on the percentages of acidic and basic amino acids (e.g. aspartic acid and histidine respectively) in mAb, the pI can be vastly different (4.6 – 9.2) as shown in Table 2. The overall charge of mAb can be tuned with the system pH relative to the pI. When pH = pI, mAb is relatively neutral in charge. At pH > pI, mAb is negatively charged and vice versa. The overall charge decides the phase behaviour of mAb in different salts. In general, the ionic specific effects on protein solubility has been reported since the late 19th century and is generally referred to as the "Hofmeister phenomena" (Fig. 7) [86–88], where cations and anions favour the solidification or dissolution of protein according to their ability to change the hydrogen bonding structure of water (conventional wisdom) or their polarizability (current opinion) [89]. For example, previous studies showed that cations had significant effect on $\Delta H_{\_crystallisation}$ (Eq. (2)) [90] and could even change the sign of $\Delta S_{\_crystallisation}$ to effect a switch from UCST to LCST behaviour [73,82,91].

Within the conventional theoretical framework, cations and anions are conventionally categorised as kosmotrope (i.e. maker of water hydrogen bonding structure) or chaotrope (i.e. breaker of water hydrogen bonding structure). Kosmotrope and chaotrope can be identified with Jones-Dole viscosity coefficient (B), which provides a direct measurement of ion–water interaction strength relative to water–water interaction strength. Kosmotropes are usually cations and anions with high charge density and tend to bind to water molecules instead of protein molecules, whereas chaotropes are usually cations and anions with low charge density and tend to bind to protein molecules instead of water molecules [87]. The Jones-Dole viscosity coefficient (B) is positive for kosmotrope and negative for chaotrope (Table in Fig. 7). The effect of cations and anions is usually reversed when switching pH from above pI to below pI as the protein surface changes from negatively charged to positively charged [88]. When pH is further away from the pI, the protein molecule is more charged and requires higher salt concentration for phase transition from solution to LLPS or precipitation or crystallisation [34,92].

As shown in Table 2, the salts investigated for mAb phase behaviour are mainly sulphates (e.g. Na_2SO_4, $(NH_4)_2SO_4$) and the sulphate ion is a moderate kosmotrope (Fig. 7) that promotes protein–protein interactions. Systematic studies of salts are still absent for mAb, especially at different pH relative to its pI. In general, when pH ~ pI, the mAb molecules are neutral in terms of surface charge. The anions follow the direct Hofmeister series, while the cations follow the inverse Hofmeister series (Fig. 7). For instance, chaotropic anions (F^-, Cl^- and SCN^-) promoted the dissolution of mAb as the ionic strength increases in the sequence of $SCN^- > Cl^- > F^-$ [69]. On the other hand, cations (Li^+ and NH_4^+) promoted the phase transition of mAb in the sequence of $Li^+ > NH_4^+$ [34,92]. At pH < pI, mAb molecules are positively charged. Anions serve as the counter ions, whereas cations serve as co-ions [88]. In general, both the anions and cations follow the inverse Hofmeister series. For instance, chaotropic anions (F^-, Cl^- and SCN^-) promoted the LLPS of protein at low concentration following the inverse Hofmeister

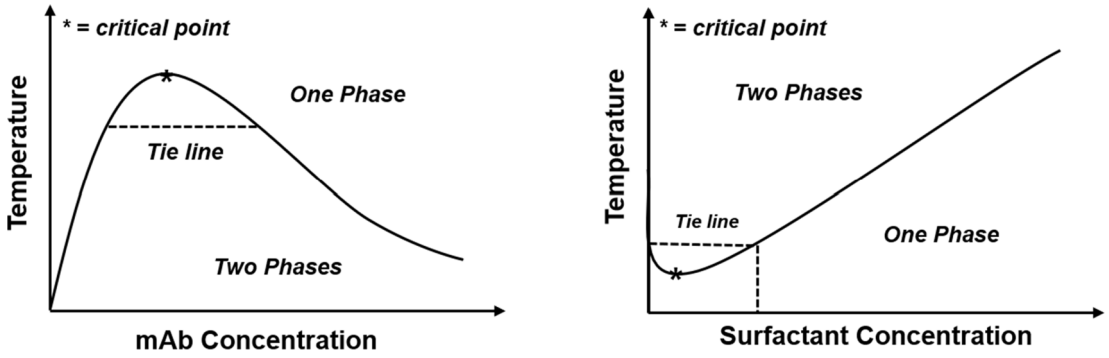

Fig. 6. Coexistence curve of mAb (left) and nonionic surfactant (right) (adapted from [50,61,69,77,78]).

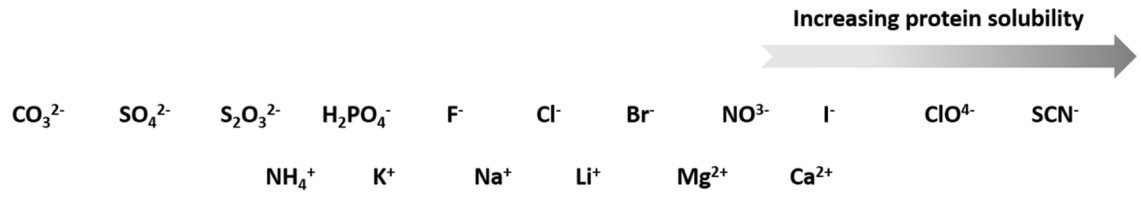

Cations	B ($dm^3 \cdot mol^{-1}$)	Anions	B ($dm^3 \cdot mol^{-1}$)
Mg^{2+}	0.39	PO_4^{3-}	0.59
Ca^{2+}	0.29	CH_3CO^{2-}	0.25
Ba^{2+}	0.22	SO_4^{2-}	0.21
Li^+	0.15	F^-	0.10
Na^+	0.09	HCO^{2-}	0.05
K^+	-0.01	Cl^-	-0.01
NH_4^+	-0.01	Br^-	-0.03
Rb^+	-0.03	NO^{3-}	-0.05
Cs^+	-0.05	ClO^{4-}	-0.06
		I^-	-0.07
		SCN^-	-0.10

Fig. 7. Hofmeister series and the corresponding Jones-Dole viscosity coefficient (B) of cation/anion (adapted from [87,89,93]).

series (i.e. $SCN^- > Cl^- > F^-$ in terms of phase transition power) [69], whereas cations (Li^+ and NH_4^+) still promoted the phase transition of mAb in the same sequence of $Li^+ > NH_4^+$ as mentioned above [34,92]. However, the specific ion effect on mAb phase transition still needs more investigation as deviation from the general trend has been reported for anions (SO_4^{2-} and Cl^-) [94].

3d. Effect of soluble polymers on phase behaviour

Soluble polymers also have significant effects on the phase behaviour of mAb and the most widely used soluble polymer is PEG [33,47,49,61,95,96]. Although other polymers such as Jeffamine were also tested [47], a more thorough study of polymer effect on mAb phase behaviour should be conducted in the future. In this review, 13 out of 20 studies on mAb phase behaviour used PEG with a wide range of molecular weight (0.4 to 20 kDa) to promote phase separation (Table 2). The depletion-attraction model is often used to explain the effect of PEG on protein phase transition [61,97,98]. In this model, the PEG molecules surround the protein molecule to form an "excluded shell" (Fig. 8 left). When two protein molecules get close to each other, their excluded shells overlap, causing the depletion of PEG molecules in the overlapped region, which results in an osmotic force that puts the protein molecules closer to each other (Fig. 8 right). The magnitude of this depletion force is influenced by the PEG concentration and the nature of protein–protein attractive force is influenced by the size ratio of PEG and protein in the form of $Rg_{\_PEG}/R_{\_protein}$, where $Rg_{\_PEG}$ is gyration radius of PEG molecule and $R_{\_protein}$ is radius of protein molecule.

When the pH is moved further away from the pI of the protein, the protein molecules are more charged and higher concentration of PEG is needed to generate the depletion force required for phase transition [99]. Furthermore, as $Rg_{\_PEG}/R_{\_protein}$ increases, the attractive force among protein molecules switches from long-range to short-range. In fact, the combination of high molecular weight PEG and salt has been used together to induce LLPS for the extraction of mAb [100–103], but the fundamental mechanisms are still not fully understood. As mAb is larger than other typical globular proteins such as lysozyme and albumin (i.e. $R_{\_mAb} > R_{\_typical\_globular\_protein}$), mAb has a lower $Rg_{\_PEG}/R_{\_protein}$ ratio than the typical globular proteins and hence the protein–protein interactions are more short-range. This means mAb requires a lower concentration of PEG to effect phase separation than the typical globular proteins.

In a study of an IgG1 phase behaviour, PEG of various molecular weights (1, 1.5, 3.35, 6 and 8 kDa) were tested for their ability to induce LLPS [61]. $Rg_{\_PEG}$ of PEG was between 1.4 and 4.3 nm, whereas $R_{\_protein}$ of the IgG1 was found to be 4.6 nm. Increasing the $Rg_{\_PEG}/R_{\_protein}$ ratio (i.e. increasing the molecular weight of PEG) and PEG concentration promoted LLPS. The tendency of LLPS had a nonlinear relationship with the mAb/PEG concentration ratio. The phase separation temperature, below which LLPS occurs, increased with the mAb/PEG concentration ratio until a maximum, after which the phase separation temperature started to decrease. At the same PEG concentration, higher mAb concentration resulted in more droplets and larger droplet size during LLPS,

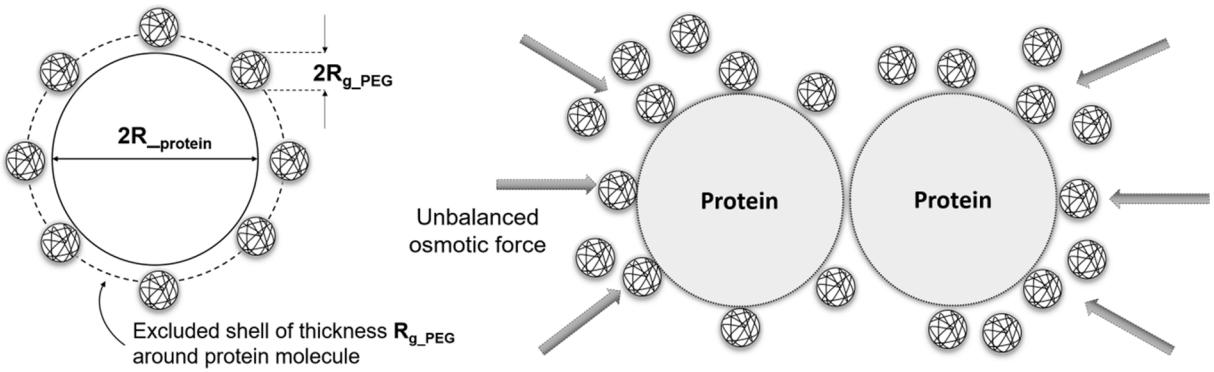

Fig. 8. Molecular interaction between PEG and mAb (adapted from [61]).

which could subsequently turn into crystals. In two other studies, good quality mAb crystals were obtained when PEGs with molecular weights of 1 – 4 kDa were used [33,47]. Since mAbs share a high degree of similarity in terms of physicochemical properties, these PEGs should be considered for mAb crystallisation in general.

4. Successful scale-ups of mAb crystallisation

The literature around successful scale-up of protein crystallisation is limited [27] and this is even more so in the case of mAb with only five reported case studies (Table 3). The two most important case studies demonstrated the crystallisation of an IgG1 from clarified cell culture at 1 L scale, showing the possibility of replacing chromatography with crystallisation for the purification of mAb [107,108]. Unlike most proteins, this IgG1 only crystallised at low ionic strength near its pI (~6.8), but the fundamental reason was unknown and should be investigated in the future. The crystallisation strategy was to reduce the salt concentration of clarified cell culture and adjust the pH to 6.8 by performing dialysis of the clarified cell culture against a 10 mM histidine/acetate buffer (pH = 5.0). It was also found that adding 2% w/v PEG 10,000 into the clarified cell culture before dialysis helped to accelerate the crystallisation, which was consistent with the findings that PEG in general promotes mAb crystallisation (Table 2). The crystallisation of IgG1 achieved a purity of 92.9% by dramatically reducing the presence of host cell protein (i.e. approx. 86% reduction) and DNA (determined by dissolving the obtained crystals and analysing the solution). Combining crystallisation and other conventional mAb processing steps such as virus inactivation, anion exchange chromatography and nanofiltration, a final purity of 99.0% could be achieved with a low host cell protein concentration (i.e. 88 ppm) and undetectable DNA concentration (i.e. < 2 ppb). On the contrary, the other three case studies demonstrated the successful scaled-up crystallisation of pure single-chain antibody and Fab fragments by using the more conventional approach of mixing the protein solutions with precipitants with high salt and PEG concentrations [109–111].

The strategy of scaling up crystallisation consists of three steps: 1) construct the phase diagram with vapour diffusion experiment to identify the crystallisation region; 2) confirm and fine-tune the crystallisation conditions with micro-batch experiments; 3) perform the crystallisation in microlitre or even litre scale [112]. The first and second steps are usually conducted with the automated high throughput method [113]. The knowledge on mAb phase behaviour mentioned in the previous section can help to identify sensible starting points and to reduce the required number of experiments to significantly increase the efficiency of the high throughput method.

In the last step (i.e. scale-up), additional aspects such as mixing, temperature control, crystal shape/size control and product removal must be considered. Mixing ensures the homogeneity of protein/precipitant concentrations and the dispersion of crystals for better control of crystal size. As shown in Table 2 and Table 3, LLPS often occurs before crystallisation for mAb and hence mixing is especially important in this case to ensure the proper dispersion of protein-rich phase in the form of droplets [109]. However, the extent of agitation must be controlled properly to avoid the denaturation of protein [114] and the breakage of crystals, which leads to secondary nucleation and more complicated crystal size control. In addition, the extent of agitation has significant influence on the crystallisation kinetics, as crystallisation was found to occur earlier in stirred tank in comparison to unstirred condition [110].

During the scale-up of crystallisation in terms of system volume, the crystallisers should maintain geometric similarity while the volume increases. Various criteria are available for determining the appropriate level of agitation, including constant minimum stirrer speed, constant impeller tip speed, constant mean power input and constant maximum local energy dissipation. It was found that maintaining a constant maximum local energy dissipation (ε_{max} in Eq. (3)) was the most suitable criterion as this approach could achieve similar crystallisation kinetics, yield, crystal size distribution and crystal shape when scaling up the process [110], whereas other criteria had problems such as the formation of crystal agglomerate and variation of crystallisation kinetics.

$$\varepsilon_{max} \approx \frac{\bar{\varepsilon} \times a}{\left(\frac{d}{D}\right)^2 \times \left(\frac{h}{d}\right)^{\frac{2}{3}} \times z^{0.6} \times (\sin\alpha)^{1.15} \times (z_I)^{\frac{2}{3}} \times \left(\frac{H}{D}\right)^{-\frac{2}{3}}} \quad (3)$$

where $\bar{\varepsilon}$ is mean power input, a is geometric parameter, d is impeller diameter, D is tank inner diameter, h is impeller height, H is tank filling height, z is number of impeller blades, z_I is number of impellers and α is blade inclination to the horizontal (Fig. 9).

Temperature control is another important aspect in mAb crystallisation, as temperature has significant influence on the phase behaviour of mAb (Table 2). In general, a combination of salting-out and cooling crystallisation can be applied to mAb as demonstrated in a case study of continuous crystallisation of IgG1 in a mixed suspension classified product removal crystalliser with tubular bypass (Fig. 10) [108]. The protein and precipitant solutions entered the crystalliser from the righthand side and were mixed instantly by the stirrer. The protein/

Table 3
Summary of successful scale-up of mAb crystallisation.

Types of mAb*	Scale	Crystallisation conditions	Observations	Ref.
IgG1	• 6 mL • 100 mL • 1L • 150 mL	• 10 mg/mL IgG1 & 20 mM NaCl in 10 mM histidine/acetate buffer (10 °C, pH = 6.8) • 25 mg/mL IgG1 & 52 mM trehalose in 10 mM histidine/acetate buffer (10 °C, pH = 6.8) • 16 mg/mL IgG1 in 10 mM histidine buffer : 80 mM TRIS base solution (10:1, v/v) as continuous feed (10 °C, pH = 6.8)	• Stirred batch crystallisation. • mAb crystallisation from clarified cell culture. • Crystallisation at low ionic strength when pH ~ pI. • Continuous crystallisation in stirred classified product removal tank with tubular reactor as bypass. • mAb crystallisation from clarified cell culture. • Crystallisation at low ionic strength when pH ~ pI.	[107] [108]
Single chain antibody	• 1 mL • 10 mL • 220 mL	• 5 mg/mL antibody & 22.5% (w/v) Na_2SO_4 & 2% (w/v) PEG 2000 & 60 mM $(NH_4)_2SO_4$ in 70 mM HEPES buffer (room temperature, pH = 7)	• Stirred batch crystallisation. • Crystallisation in the sulphate-rich phase and near the boundary of droplet during liquid–liquid phase separation. • Crystals accumulated in the PEG-rich phase when the stirring stopped and the mixture separated into two layers (PEG-rich phase on top).	[109]
Fab fragment of canakinumab	• 6 mL	• 3 mg/mL Fab fragment & 14% PEG 5000 & 100 mM NaCl in 50 mM in sodium malonate buffer (28 °C, pH = 7.0)	• Stirred batch crystallisation. • Crystallisation appeared four times after under stirring than unstirred condition.	[110]
Fab fragment	• 5 mL • 100 mL	• 110 mg/mL Fab fragment & 1.1 – 1.6 M $(NH_4)_2SO_4$ in 40 mM sodium citrate buffer (20 °C, pH = 6.25).	• Stirred batch crystallisation. • Increasing concentration of $(NH_4)_2SO_4$ to drive the crystallisation yield to 99%.	[111]

* Intact unless stated otherwise.

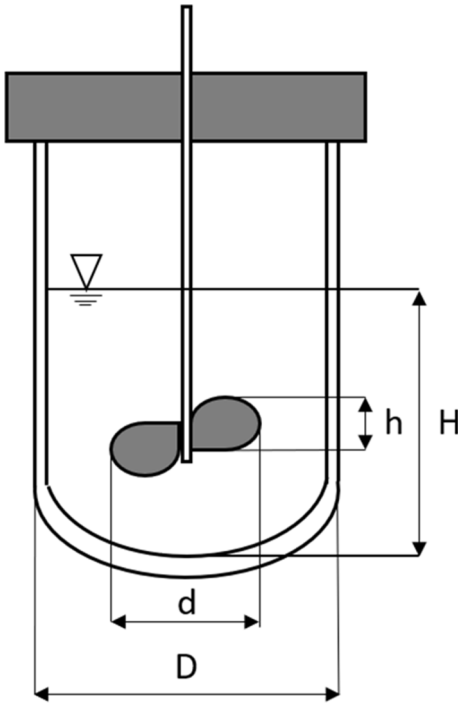

Fig. 9. Typical stirred tank with blade impeller.

precipitant mixture was pumped into the tubular bypass that was maintained at a lower temperature to initiate nucleation. Using the tubular bypass increased process flexibility as nucleation was decoupled from crystal growth that mainly took place in the stirred tank. In the case study, the main stirred tank was operated in batch mode without the bypass for two hours to initiate the crystallisation, before the system was switched to the continuous mode, where IgG1/tris mixture entered the main tank continuously and IgG1 crystals were continuously removed from the bottom of the tank. The main tank was maintained at 10 °C, whereas the bypass was maintained at 0 °C (note: the main tank temperature was controlled by the temperature and flow rate of the stream leaving the bypass and returning to the tank). At steady state, high yield and purity were achieved (93% & 96% respectively).

Based on the limited case studies summarised in Table 3, it is obvious that mAb crystallisation still has a long way to go. The demand for cost-effective biosimilars of mAb-based therapeutics in the next few decades provides a strong motivation for the development of mAb crystallisation for purification purposes. A proposed purification process flow chart is shown in Fig. 11 (right), where the chromatographic steps in the conventional mAb manufacturing (Fig. 11 (left)) is replaced by two crystallisation steps to achieve high purity.

As purification cost usually accounts for >50% of the entire

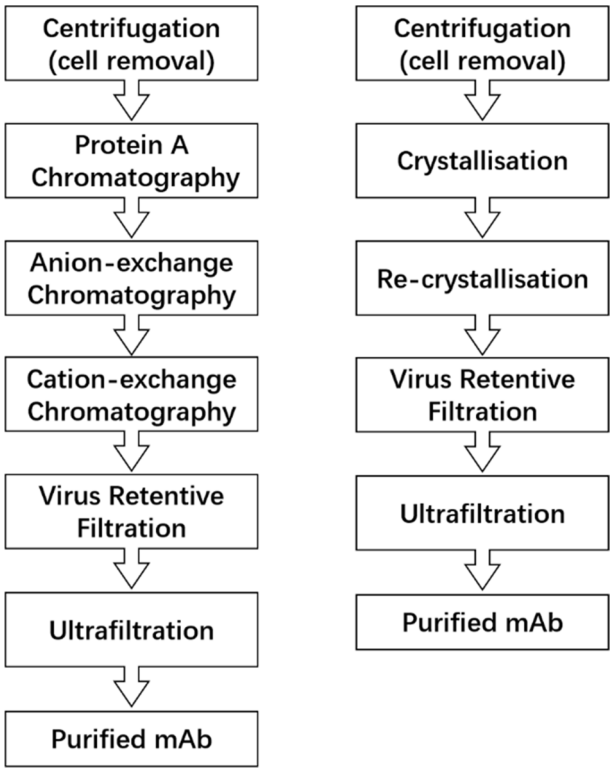

Fig. 11. Purification process flow chart for (left) conventional mAb manufacturing and (right) with replacement of chromatography with crystallisation.

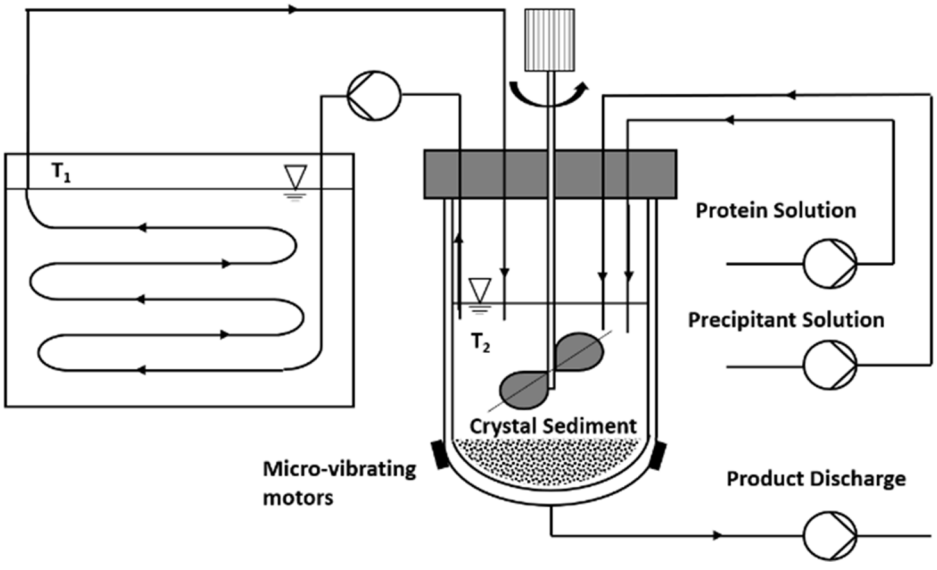

Fig. 10. Mixed suspension classified product removal crystalliser with tubular bypass (adapted from [108]).

production cost and affinity chromatography (i.e. with protein-A resin) accounts for ~70% of the overall purification cost [6,10,11], the successful replacement of affinity chromatography with crystallisation can achieve a substantial reduction (i.e. ~20 – 30%) in the production cost of mAb-based therapeutics (note: this estimate is agreed by industrial producers of mAb that we have collaborated with over the past few years), which will subsequently translate into more affordable therapeutics and less heavy financial burdens for patients. In terms of scale, crystallisation can be conducted in industrial bioreactors where the synthesis of mAb takes place. These bioreactors have volume normally between a few hundred to approximately ten thousand litres and the typical titre is ~10 g/L [6,10,11]. This means crystallisation can process up to 100 kg mAb per batch in a 10,000 L bioreactor.

The key impurities for removal are host cell proteins, DNA and virus (Fig. 2 (left)), which are the by-products of the mAb synthesis by mammalian cells. Due to the different physicochemical properties of these impurities, the purification of mAb is a complex process [115]. For example, the host cell proteins consist of multiple proteins that have a wide range of molecular weight and pI. For instance, in a previous study of mAb production with CHO cells, more than 20 types of host cell proteins were detected with molecular weights between 22 and 406 kDa and pI between 4.4 and 11.0 [116]. On the other hand, DNA and virus (e.g. minute virus of mice) have relatively more predictable size (e.g. ~25 nm for minute virus of mice) [117] and pI (~5 for DNA and minute virus of mice) [118,119]. The diverse physicochemical properties of impurities significantly increase the complexity of mAb purification because they not only exist as individual components, but also associate with the mAb molecules. For example, previous studies have investigated the association of host cell protein with mAb [116,120,121]. As such two more chromatographic steps are necessary after the Protein-A chromatography (i.e. affinity chromatography) in the conventional practice (Fig. 11 (left)). In the context of mAb crystallisation (Fig. 11 (right)), this means the screening of crystallisation conditions must consider suitable experimental conditions (i.e. pH, temperature and additives) that favours the dissociation of impurities from mAb.

Over the past decade, although significant advances have been made on the understanding of fundamental mechanisms of crystallisation [122–124], the development of heterogeneous/homogeneous templates to enhance the crystallisation [12,125–132] as well as the process development of protein crystallisation [112,114,133,134], a number of areas still require more research attention for the incorporation of mAb crystallisation into pharmaceutical manufacturing, including:

1) Crystal properties characterisation;
2) Crystal shape control;
3) Heterogeneous crystallisation;
4) Continuous crystallisation.

Firstly, the physical and chemical properties of mAb crystals are rarely available in literature, but they are important for the handling of mAb crystals during manufacturing. For example, the mechanical strength of mAb crystal determines the suitable shear stress produced by agitation to avoid or promote the breakage of mAb crystals in a crystalliser. Secondly, shape control is still largely unexplored for mAb crystals, but crucial in the manufacturing process. In most of the previous studies, mAb crystals appeared in needle shape [46], which is undesirable for processing as needle crystals tend to block pipes and filters. With mAb crystals properly characterised (i.e. point 1 above), the growth rate of different facets under different experimental conditions can be determined and manipulated accurately for achieving the desirable crystal shape. Thirdly, the development of heterogeneous nucleants for protein crystallisation is one of the latest developments in this area [135–143]. Previous studies have shown that physiochemical properties of heterogeneous nucleants that are important for enhancing protein crystallisation include pore size and surface chemistry [125,129,144]. The development of suitable heterogeneous nucleants for mAb is an important direction, especially in achieving selective crystallisation of mAb in the presence of biological impurities. Lastly, continuous crystallisation for mAb is advantageous in terms of scalability and product quality consistency and hence more research effort should be directed to this area. Previous studies have demonstrated that various crystalliser configurations (i.e. stirred tank, tubular, membrane) can be used to crystallise proteins [27,108,112,145–148]. In the case of mAb, the process fluid is significantly more viscous than water due to the use of PEG as a crystallising additive. As a result, ensuring proper mixing can be tricky in stirred tank crystalliser that uses impeller for mixing and in conventional tubular crystalliser that relies on high flow rate for creating turbulence, as a previous study showed that protein could be denatured under moderate shear stress [114]. In our opinion, tubular crystallisers coupled with oscillatory flow or slug flow might be better options for the continuous crystallisation of mAb, but more experimental studies must be conducted in the future for validation.

5. Conclusion

Compare with small molecule compounds, protein is challenging to crystallise due to the large and complex nature of protein molecules. mAb is even more difficult to crystallise than conventional globular proteins such as lysozyme because of its significantly larger molecular weight (i.e. 150 kDa vs 15 kDa of lysozyme) and high flexibility due to the presence of hinge region that connects Fab and Fc. Although therapeutically relevant mAb are highly similar in terms of molecular shape (i.e. Y-shape) and amino acid sequence, slight changes in the amino acid sequence of the variable domain can result in significant changes of pI and tremendous implications for the phase behaviour in the presence of salts. An overview of the studies conducted on the phase behaviour of mAb shows that the pI of mAb (IgG1) covered a wide range (i.e. 4.7–9.2) and the effect of ions could follow a completely trend (i.e. direct vs inverse Hoffmeister series) at the same pH. Crystallisation of mAb was often observed with LLPS, as the protein-rich phase could have as high as 100 folds of protein enrichment as compared with the protein-poor phase. PEG are the most popular macromolecules used to induce LLPS and subsequently the crystallisation of mAb as they tends to enhance the short-range interaction between mAb molecules and hence the chances of crystallisation. Due to the limited understanding of the mechanisms of LLPS and crystallisation of mAb, the number of successful demonstrations of mAb crystallisation scale-up is limited. The existing demonstrations showed that mAb could be directly crystallised from clarified cell culture and crystallisation could replace chromatography to achieve high yield and purity. However, more efforts are needed to understand the interactions between impurities (i.e. host cell proteins, DNA and virus) and mAb in order to identify suitable crystallisation conditions. When scaling up crystallisation, mixing and temperature control are two critical factors to be considered. Existing demonstrations show that maintaining a constant maximum local energy dissipation is the most suitable scale-up criteria for mixing and combining a cooling by-pass with a stirred tank crystalliser as a temperature control strategy can decouple nucleation and crystal growth and significantly increases process flexibility.

Declaration of Competing Interest

The authors declare that they have no known competing financial interests or personal relationships that could have appeared to influence the work reported in this paper.

Acknowledgement

The financial support of this work comes from the SCoBiC project which is funded by the UK's EPSRC (EP/N015916/1).

References

[1] B. Nagel, H. Dellweg, L.M. Gierasch, Glossary for chemists of terms used in biotechnology, Pure Appl. Chem. 64 (1992) 143–168.
[2] P. Chames, M. Van Regenmortel, E. Weiss, D. Baty, Therapeutic antibodies: Successes, limitations and hopes for the future, Br. J. Pharmacol. 157 (2009) 220–233.
[3] Z. Elgundi, M. Reslan, E. Cruz, V. Sifniotis, V. Kayser, The state-of-play and future of antibody therapeutics, Adv. Drug Deliv. Rev. 122 (2017) 2–19.
[4] R. O'Kennedy, C. Murphy, T. Devine, Technology advancements in antibody purification, Antib. Technol. J. 6 (2016) 17–32.
[5] G. Walsh, Biopharmaceutical benchmarks 2018, Nat. Biotechnol. 36 (2018) 1136–1145, https://doi.org/10.1038/nbt.4305.
[6] B. Kelley, Industrialization of mAb production technology: The bioprocessing industry at a crossroads, MAbs. 1 (2009) 440–449.
[7] U. Gottschalk, Process Scale Purification of Antibodies (2008).
[8] H.F. Liu, J. Ma, C. Winter, R. Bayer, Recovery and purification process development for monoclonal antibody production, MAbs. 2 (2010) 480–499.
[9] D.M. Ecker, S.D. Jones, H.L. Levine, The therapeutic monoclonal antibody market, MAbs. 7 (2015) 9–14.
[10] S.S. Farid, Process economics of industrial monoclonal antibody manufacture, J. Chromatogr. B Anal. Technol. Biomed, Life Sci. 848 (2007) 8–18.
[11] N. Hammerschmidt, A. Tscheliessnig, R. Sommer, B. Helk, A. Jungbauer, Economics of recombinant antibody production processes at various scales: Industry-standard compared to continuous precipitation, Biotechnol. J. 9 (2014) 766–775.
[12] W. Chen, T.N.H. Cheng, L.F. Khaw, X. Li, H. Yang, J. Ouyang, J.Y.Y. Heng, Protein purification with nanoparticle-enhanced crystallisation, Sep. Purif. Technol. 255 (2020), 117384, https://doi.org/10.1016/j.seppur.2020.117384.
[13] A. Navarro, H.S. Wu, S.S. Wang, Engineering problems in protein crystallization, Sep. Purif. Technol. 68 (2009) 129–137.
[14] X. He, R. Chen, X. Zhu, Q. Liao, S. Li, Laser assisted microfluidic membrane evaporator for sample crystallization separation, Sep. Purif. Technol. 242 (2020), 116817.
[15] Z. Ding, S. Li, X. Cao, Separation of lysozyme from salted duck egg white by affinity precipitation using pH-responsive polymer with an L-thyroxin ligand, Sep. Purif. Technol. 138 (2014) 153–160.
[16] K.J. Hwang, H.C. Hwang, The purification of protein in cross-flow microfiltration of microbe/protein mixtures, Sep. Purif. Technol. 51 (2006) 416–423.
[17] Y. Wan, J. Lu, Z. Cui, Separation of lysozyme from chicken egg white using ultrafiltration, Sep. Purif. Technol. 48 (2006) 133–142.
[18] N. Alele, M. Ulbricht, Membrane-based purification of proteins from nanoparticle dispersions: Influences of membrane type and ultrafiltration conditions, Sep. Purif. Technol. 158 (2016) 171–182.
[19] F.A. Van Winssen, J. Merz, L.M. Czerwonka, G. Schembecker, T. Dortmund, Application of the Tunable Aqueous Polymer-Phase Impregnated Resins-Technology for protein purification, Sep. Purif. Technol. 136 (2014) 123–129.
[20] G. Ren, X. Gong, B. Wang, Y. Chen, J. Huang, Affinity ionic liquids for the rapid liquid-liquid extraction purification of hexahistidine tagged proteins, Sep. Purif. Technol. 146 (2015) 114–120.
[21] S.C. Lo, R.N. Ramanan, B.T. Tey, W.S. Tan, P.L. Show, T.C. Ling, C.W. Ooi, Purification of the recombinant enhanced green fluorescent protein from Escherichia coli using alcohol + salt aqueous two-phase systems, Sep. Purif. Technol. 192 (2018) 130–139.
[22] L.S. Castro, P. Pereira, L.A. Passarinha, M.G. Freire, A.Q. Pedro, Enhanced performance of polymer-polymer aqueous two-phase systems using ionic liquids as adjuvants towards the purification of recombinant proteins, Sep. Purif. Technol. 248 (2020), 117051.
[23] D.C.V. Belchior, M.V. Quental, M.M. Pereira, C.M.N. Mendonça, I.F. Duarte, M. G. Freire, Performance of tetraalkylammonium-based ionic liquids as constituents of aqueous biphasic systems in the extraction of ovalbumin and lysozyme, Sep. Purif. Technol. 233 (2020), 116019.
[24] A.A. Shukla, L.S. Wolfe, S.S. Mostafa, C. Norman, Evolving trends in mAb production processes, Bioeng. Transl. Med. 2 (2017) 58–69.
[25] A.C.A. Roque, A.S. Pina, A.M. Azevedo, R. Aires-Barros, A. Jungbauer, G. Di Profio, J.Y.Y. Heng, J. Haigh, M. Ottens, Anything but Conventional Chromatography Approaches in Bioseparation, Biotechnol. J. 15 (2020) 1900274.
[26] S.L. Morissette, Ö. Almarsson, M.L. Peterson, J.F. Remenar, M.J. Read, A. V. Lemmo, S. Ellis, M.J. Cima, C.R. Gardner, High-throughput crystallization: Polymorphs, salts, co-crystals and solvates of pharmaceutical solids, Adv. Drug Deliv. Rev. 56 (2004) 275–300.
[27] W. Chen, H. Yang, J.Y.Y. Heng, Continuous Protein Crystallization, in: Handb. Contin. Cryst., 2020: pp. 372–392, https://doi.org/10.1039/9781788013581-00372.
[28] D. Hekmat, Large-scale crystallization of proteins for purification and formulation, Bioprocess Biosyst. Eng. 38 (2015) 1209–1231.
[29] M.J. Feige, M.A. Gräwert, M. Marcinowski, J. Hennig, J. Behnke, D. Auslander, E. M. Heroldb, J. Peschek, C.D. Castrod, M. Flajnik, L.M. Hendershot, M. Sattler, M. Grollb, J. Buchner, The structural analysis of shark IgNAR antibodies reveals evolutionary principles of immunoglobulins, Proc. Natl. Acad. Sci. U. S. A. 111 (2014) 8155–8160, https://doi.org/10.1073/pnas.1321502111.
[30] G. Köhler, C. Milstein, Continuous cultures of fused cells secreting antibody of predefined specificity, Nature. 256 (1975) 495–497.
[31] T. Ahamed, B.N.A. Esteban, M. Ottens, G.W.K. Van Dedem, L.A.M. Van Der Wielen, M.A.T. Bisschops, A. Lee, C. Pham, J. Thömmesy, Phase behavior of an intact monoclonal antibody, Biophys. J. 93 (2007) 610–619.
[32] M.T. Schermeyer, A.K. Wöll, B. Kokke, M. Eppink, J. Hubbuch, Characterization of highly concentrated antibody solution - A toolbox for the description of protein long-term solution stability, MAbs. 9 (2017) 1169–1185.
[33] N. Rakel, L. Galm, K.C. Bauer, J. Hubbuch, Influence of macromolecular precipitants on phase behavior of monoclonal antibodies, Biotechnol. Prog. 31 (2015) 145–153.
[34] N. Rakel, K.C. Bauer, L. Galm, J. Hubbuch, From osmotic second virial coefficient (B22) to phase behavior of a monoclonal antibody, Biotechnol. Prog. 31 (2015) 438–451.
[35] E. Pantuso, T.F. Mastropietro, M.L. Briuglia, C.J.J. Gerard, E. Curcio, J.H. ter Horst, F.P. Nicoletta, G. Di Profio, On the Aggregation and Nucleation Mechanism of the Monoclonal Antibody Anti-CD20 Near Liquid-Liquid Phase Separation (LLPS), Sci. Rep. 10 (2020) 1–14, https://doi.org/10.1038/s41598-020-65776-6.
[36] R.A. Lewus, P.A. Darcy, A.M. Lenhoff, S.I. Sandler, Interactions and phase behavior of a monoclonal antibody, Biotechnol. Prog. 27 (2011) 280–289.
[37] A. George, W.W. Wilson, Predicting protein crystallization from a dilute solution property, Acta Crystallogr. Sect. D Biol. Crystallogr. 50 (1994) 361–365.
[38] C. Haas, J. Drenth, The protein-water phase diagram and the growth of protein crystals from aqueous solution, J. Phys. Chem. B. 102 (1998) 4226–4232, https://doi.org/10.1021/jp980296j.
[39] R.C. Stevens, High-throughput protein crystallization, Curr. Opin. Struct. Biol. 10 (2000) 558–563.
[40] S. Yadav, S.J. Shire, D.S. Kalonia, Viscosity analysis of high concentration bovine serum albumin aqueous solutions, Pharm. Res. 28 (2011) 1973–1983.
[41] M.T. Schermeyer, H. Sigloch, K.C. Bauer, C. Oelschlaeger, J. Hubbuch, Squeeze flow rheometry as a novel tool for the characterization of highly concentrated protein solutions, Biotechnol. Bioeng. 113 (2016) 576–587.
[42] H. Hasegawa, J. Wendling, F. He, E. Trilisky, R. Stevenson, H. Franey, F. Kinderman, G. Li, D.M. Piedmonte, T. Osslund, M. Shen, R.R. Ketchem, In vivo crystallization of human IgG in the endoplasmic reticulum of engineered chinese hamster ovary (CHO) cells, J. Biol. Chem. 286 (2011) 19917–19931.
[43] S. Chen, H. Lau, Y. Brodsky, G.R. Kleemann, R.F. Latypov, The use of native cation-exchange chromatography to study aggregation and phase separation of monoclonal antibodies, Protein Sci. 19 (2010) 1191–1204.
[44] J.W. Mullin, Crystallization, Elsevier, 2001, https://books.google.co.uk/books?hl=en&lr=&id=Et0EtojQmvsC&oi=fnd&pg=PP1&dq=J.W.+Mullin,+Crystallization,+Elsevier,+2001.&ots=Vt7x4YLAuL&sig=egABhW-1N4h1vxlsjCtZjTRoV_0&redir_esc=y#v=onepage&q=J.W.%20Mullin%2C%20Crystallization%2C%20Elsevier%2C%202001.&f=false.
[45] C. Haas, J. Drenth, Understanding protein crystallization on the basis of the phase diagram, J. Cryst. Growth. 196 (1999) 388–394.
[46] H. Yang, B.D. Belviso, X. Li, W. Chen, T. Mastropietro, G. Di Profio, R. Caliandro, J.Y.Y. Heng, Optimization of vapor diffusion conditions for anti-CD20 crystallization and scale-up to meso batch, Crystals. 9 (2019) 230, https://doi.org/10.3390/cryst9050230.
[47] Y.G. Kuznetsov, A.J. Malkin, A. McPherson, The liquid protein phase in crystallization: A case study - Intact immunoglobulins, J. Cryst. Growth. 232 (2001) 30–39.
[48] P.G. Vekilov, Phase transitions of folded proteins, Soft Matter. 6 (2010) 5254–5272.
[49] Y. Wang, A. Lomakin, R.F. Latypov, J.P. Laubach, T. Hideshima, P.G. Richardson, N.C. Munshi, K.C. Anderson, G.B. Benedek, Phase transitions in human IgG solutions, J. Chem. Phys. 139 (2013), 121904, https://doi.org/10.1063/1.4811345.
[50] H. Nishi, M. Miyajima, H. Nakagami, M. Noda, S. Uchiyama, K. Fukui, Phase separation of an IgG1 antibody solution under a low ionic strength condition, Pharm. Res. 27 (2010) 1348–1360.
[51] Y. Wang, A. Lomakin, R.F. Latypov, G.B. Benedek, Phase separation in solutions of monoclonal antibodies and the effect of human serum albumin, Proc. Natl. Acad. Sci. 108 (2011) 16606–16611.
[52] D. Leckband, J. Israelachvili, Intermolecular forces in biology, Q. Rev. Biophys. 34 (2001) 105–267, https://doi.org/10.1017/S0033583501003687.
[53] A. Paliwal, D. Asthagiri, D. Abras, A.M. Lenhoff, M.E. Paulaitis, Light-scattering studies of protein solutions: Role of hydration in weak protein-protein interactions, Biophys. J. 89 (2005) 1564–1573.
[54] D.E. Kuehner, C. Heyer, C. Rämsch, U.M. Fornefeld, H.W. Blanch, J.M. Prausnitz, Interactions of lysozyme in concentrated electrolyte solutions from dynamic light-scattering measurements, Biophys. J. 73 (1997) 3211–3224.
[55] A. McPherson, B. Cudney, Searching for silver bullets: An alternative strategy for crystallizing macromolecules, J. Struct. Biol. 156 (2006) 387–406.
[56] A.C. Dumetz, A.M. Snellinger-O'Brien, E.W. Kaler, A.M. Lenhoff, Patterns of protein-protein interactions in salt solutions and implications for protein crystallization, Protein Sci. 16 (2007) 1867–1877, https://doi.org/10.1110/ps.072957907.
[57] O.D. Velev, E.W. Kaler, A.M. Lenhoff, Protein interactions in solution characterized by light and neutron scattering: Comparison of lysozyme and chymotrypsinogen, Biophys. J. 75 (1998) 2682–2697.
[58] X. Song, X. Zhao, The van der Waals interaction between protein molecules in an electrolyte solution, J. Chem. Phys. 120 (2004) 2005–2009, https://doi.org/10.1063/1.1634955.
[59] M. Muschol, F. Rosenberger, Interactions in undersaturated and supersaturated lysozyme solutions: Static and dynamic light scattering results, J. Chem. Phys. 103 (1995) 10424–10432, https://doi.org/10.1063/1.469891.
[60] C.J. Coen, J. Newman, H.W. Blanch, J.M. Prausnitz, Electrostatic protein-protein interactions: Comparison of point-dipole and finite-length dipole potentials of mean force, J. Colloid Interface Sci. 177 (1996) 276–279.

[61] A.I. Jion, L.T. Goh, S.K.W. Oh, Crystallization of IgG1 by mapping its liquid-liquid phase separation curves, Biotechnol. Bioeng. 95 (2006) 911–918.
[62] C. Haas, J. Drenth, The Interface between a Protein Crystal and an Aqueous Solution and Its Effects on Nucleation and Crystal Growth, J. Phys. Chem. B. 104 (2000) 368–377, https://doi.org/10.1021/jp993210a.
[63] P.R. Ten Wolde, D. Frenkel, Enhancement of protein crystal nucleation by critical density fluctuations, Science. 277 (1997) 1975–1978, https://doi.org/10.1126/science.277.5334.1975.
[64] V.J. Anderson, H.N.W. Lekkerkerker, Insights into phase transition kinetics from colloid science, Nature. 416 (2002) 811–815, https://doi.org/10.1038/416811a.
[65] N. Wentzel, J.D. Gunton, Effect of solvent on the phase diagram of a simple anisotropic model of globular proteins, J. Phys. Chem. B. 112 (2008) 7803–7809.
[66] M. Muschol, F. Rosenberger, Liquid-liquid phase separation in supersaturated lysozyme solutions and associated precipitate formation/crystallization, J. Chem. Phys. 107 (1997) 1953–1962, https://doi.org/10.1063/1.474547.
[67] H. Shirahama, J. Lyklema, W. Norde, Comparative protein adsorption in model systems, J. Colloid Interface Sci. 139 (1990) 177–187.
[68] Y.I. Tarasevich, Interaction of globular albumins with the silica surface, Theor. Exp. Chem. 37 (2001) 98–102, https://doi.org/10.1023/A:1010453409208.
[69] B.D. Mason, J. Zhang-Van Enk, L. Zhang, R.L. Remmele, J. Zhang, Liquid-liquid phase separation of a monoclonal antibody and nonmonotonic influence of Hofmeister anions, Biophys. J. 99 (2010) 3792–3800.
[70] V.G. Taratuta, A. Holschbach, G.M. Thurston, D. Blankschtein, G.B. Benedek, Liquid-liquid phase separation of aqueous lysozyme solutions: Effects of pH and salt identity, J. Phys. Chem. 94 (1990) 2140–2144.
[71] W.D. Terry, B.W. Matthews, D.R. Davies, Crystallographic studies of a human immunoglobulin, Nature. 220 (1968) 239–241.
[72] A.B. Edmundson, M.K. Wood, M. Schiffer, K.D. Hardman, C.F. Ainsworth, K. R. Ely, A crystallographic investigation of a human IgG immunoglobulin, J. Biol. Chem. 245 (1970) 2763–2764.
[73] F. Zhang, R. Roth, M. Wolf, F. Roosen-Runge, M.W.A. Skoda, R.M.J. Jacobs, M. Stzucki, F. Schreiber, Charge-controlled metastable liquid-liquid phase separation in protein solutions as a universal pathway towards crystallization, Soft Matter. 8 (2012) 1313–1316, https://doi.org/10.1039/C2SM07008A.
[74] O. Galkin, P.G. Vekilov, Control of protein crystal nucleation around the metastable liquid-liquid phase boundary, Proc. Natl. Acad. Sci. U. S. A. 97 (2000) 6277–6281, https://doi.org/10.1073/pnas.110000497.
[75] W.J. Ray, C.E. Bracker, Polyethylene glycol: Catalytic effect on the crystallization of phosphoglucomutase at high salt concentration, J. Cryst. Growth. 76 (1986) 562–576.
[76] C. Gripon, L. Legrand, I. Rosenman, O. Vidal, M.C. Robert, F. Boué, Lysozyme solubility in H2O and D2O solutions: A simple relationship, J. Cryst. Growth. 177 (1997) 238–247.
[77] A.M. Lopes, V.D.C. Santos-Ebinuma, L.C.D.L. Novaes, J.V.D. Molino, L.R. S. Barbosa, A. Pessoa, C.D.O. Rangel-Yagui, LPS-protein aggregation influences protein partitioning in aqueous two-phase micellar systems, Appl. Microbiol. Biotechnol. 97 (2013) 6201–6209.
[78] P. Timmins, E. Pebay-Peyroula, W. Welte, Detergent organisation in solutions and in crystals of membrane proteins, Biophys. Chem. 53 (1994) 27–36.
[79] S.T. Yau, D.N. Petsev, B.R. Thomas, P.G. Vekilov, Molecular-level thermodynamic and kinetic parameters for the self-assembly of apoferritin molecules into crystals, J. Mol. Biol. 303 (2000) 667–678.
[80] O. Gliko, W. Pan, P. Katsonis, N. Neumaier, O. Galkin, S. Weinkauf, P.G. Vekilov, Metastable liquid clusters in super- and undersaturated protein solutions, J. Phys. Chem. B. 111 (2007) 3106–3114.
[81] P.G. Vekilov, A.R. Feeling-Taylor, D.N. Petsev, O. Galkin, R.L. Nagel, R.E. Hirsch, Intermolecular interactions, nucleation, and thermodynamics of crystallization of hemoglobin C, Biophys. J. 83 (2002) 1147–1156.
[82] O. Matsarskaia, M.K. Braun, F. Roosen-Runge, M. Wolf, F. Zhang, R. Roth, F. Schreiber, Cation-Induced Hydration Effects Cause Lower Critical Solution Temperature Behavior in Protein Solutions, J. Phys. Chem. B. 120 (2016) 7731–7736.
[83] M. Kastelic, Y.V. Kalyuzhnyi, B. Hribar-Lee, K.A. Dil, V. Vlachy, Protein aggregation in salt solutions, Proc. Natl. Acad. Sci. U. S. A. 112 (2015) 6766–6770.
[84] R. Gupta, R. Mauri, R. Shinnar, Phase separation of liquid mixtures in the presence of surfactants, Ind. Eng. Chem. Res. 38 (1999) 2418–2424, https://doi.org/10.1021/ie9807699.
[85] A.L. Grilo, M.R. Aires-Barros, A.M. Azevedo, Partitioning in Aqueous Two-Phase Systems: Fundamentals, Applications and Trends, Sep. Purif. Rev. 45 (2016) 68–80.
[86] W. Kunz, J. Henle, B.W. Ninham, "Zur Lehre von der Wirkung der Salze" (about the science of the effect of salts): Franz Hofmeister's historical papers, Curr. Opin. Colloid Interface Sci. 9 (2004) 19–37.
[87] K.D. Collins, Ions from the Hofmeister series and osmolytes: Effects on proteins in solution and in the crystallization process, Methods. 34 (2004) 300–311.
[88] M. Boström, F.W. Tavares, S. Finet, F. Skouri-Panet, A. Tardieu, B.W. Ninham, Why forces between proteins follow different Hofmeister series for pH above and below pI, Biophys. Chem. 117 (2005) 217–224.
[89] Y. Zhang, P.S. Cremer, Interactions between macromolecules and ions: the Hofmeister series, Curr. Opin. Chem. Biol. 10 (2006) 658–663.
[90] P. Bénas, L. Legrand, M. Riès-Kautt, Strong and specific effects of cations on lysozyme chloride solubility, Acta Crystallogr. Sect. D Biol. Crystallogr. 58 (2002) 1582–1587, https://doi.org/10.1107/S0907444902014518.
[91] M.K. Braun, M. Wolf, O. Matsarskaia, S. Da Vela, F. Roosen-Runge, M. Sztucki, R. Roth, F. Zhang, F. Schreiber, Strong Isotope Effects on Effective Interactions and Phase Behavior in Protein Solutions in the Presence of Multivalent Ions, J. Phys. Chem. B. 121 (2017) 1731–1739.
[92] R.A. Lewus, N.E. Levy, A.M. Lenhoff, S.I. Sandler, A comparative study of monoclonal antibodies. 1. phase behavior and protein-protein interactions, Biotechnol. Prog. 31 (2015) 268–276.
[93] H.I. Okur, J. Hladílková, K.B. Rembert, Y. Cho, J. Heyda, J. Dzubiella, P. S. Cremer, P. Jungwirth, Beyond the Hofmeister Series: Ion-Specific Effects on Proteins and Their Biological Functions, J. Phys. Chem. B. 121 (2017) 1997–2014.
[94] N. Rakel, M. Baum, J. Hubbuch, Moving through three-dimensional phase diagrams of monoclonal antibodies, Biotechnol. Prog. 30 (2014) 1103–1113.
[95] L.J. Harris, E. Skaletsky, A. McPherson, Crystallization of intact monoclonal antibodies, Proteins Struct. Funct. Bioinforma. 23 (1995) 285–289.
[96] Y. Wang, R.F. Latypov, A. Lomakin, J.A. Meyer, B.A. Kerwin, S. Vunnum, G. B. Benedek, Quantitative evaluation of colloidal stability of antibody solutions using PEG-induced liquid-liquid phase separation, Mol. Pharm. 11 (2014) 1391–1402.
[97] S. Asakura, F. Oosawa, On interaction between two bodies immersed in a solution of macromolecules, J. Chem. Phys. 22 (1954) 1255–1256.
[98] S. Asakura, F. Oosawa, Interaction between particles suspended in solutions of macromolecules, J. Polym. Sci. 33 (1958) 183–192.
[99] R.W. Thompson, R.F. Latypov, Y. Wang, A. Lomakin, J.A. Meyer, S. Vunnum, G. B. Benedek, Evaluation of effects of pH and ionic strength on colloidal stability of IgG solutions by PEG-induced liquid-liquid phase separation, J. Chem. Phys. 145 (2016), 185101.
[100] B.A. Andrews, S. Nielsen, J.A. Asenjo, Partitioning and purification of monoclonal antibodies in aqueous two-phase systems, Bioseparation. 6 (1996) 303–313. https://europepmc.org/article/med/9210350.
[101] A.M. Azevedo, P.A.J. Rosa, I.F. Ferreira, M.R. Aires-Barros, Optimisation of aqueous two-phase extraction of human antibodies, J. Biotechnol. 132 (2007) 209–217.
[102] M.F.F. Silva, A. Fernandes-Platzgummer, M.R. Aires-Barros, A.M. Azevedo, Integrated purification of monoclonal antibodies directly from cell culture medium with aqueous two-phase systems, Sep. Purif. Technol. 132 (2014) 330–335.
[103] A.M. Azevedo, P.A.J. Rosa, I.F. Ferreira, M.R. Aires-Barros, Chromatography-free recovery of biopharmaceuticals through aqueous two-phase processing, Trends Biotechnol. 27 (2009) 240–247.
[104] E. Trilisky, R. Gillespie, T.D. Osslund, S. Vunnum, Crystallization and liquid-liquid phase separation of monoclonal antibodies and fc-fusion proteins: Screening results, Biotechnol. Prog. 27 (2011) 1054–1067.
[105] Y. Zang, B. Kammerer, M. Eisenkolb, K. Lohr, H. Kiefer, Towards protein crystallization as a process step in downstream processing of therapeutic antibodies: Screening and optimization at microbatch scale, PLoS One. 6 (2011), e25282.
[106] K. Reiche, J. Hartl, A. Blume, P. Garidel, Liquid-liquid phase separation of a monoclonal antibody at low ionic strength: Influence of anion charge and concentration, Biophys. Chem. 220 (2017) 7–19.
[107] B. Smejkal, N.J. Agrawal, B. Helk, H. Schulz, M. Giffard, M. Mechelke, F. Ortner, P. Heckmeier, B.L. Trout, D. Hekmat, Fast and scalable purification of a therapeutic full-length antibody based on process crystallization, Biotechnol. Bioeng. 110 (2013) 2452–2461.
[108] D. Hekmat, M. Huber, C. Lohse, N. Von Den Eichen, D. Weuster-Botz, Continuous Crystallization of Proteins in a Stirred Classified Product Removal Tank with a Tubular Reactor in Bypass, Cryst. Growth Des. 17 (2017) 4162–4169.
[109] H. Huettmann, M. Berkemeyer, W. Buchinger, A. Jungbauer, Preparative crystallization of a single chain antibody using an aqueous two-phase system, Biotechnol. Bioeng. 111 (2014) 2192–2199.
[110] B. Smejkal, B. Helk, J.M. Rondeau, S. Anton, A. Wilke, P. Scheyerer, J. Fries, D. Hekmat, D. Weuster-Botz, Protein crystallization in stirred systems-scale-up via the maximum local energy dissipation, Biotechnol. Bioeng. 110 (2013) 1956–1963.
[111] D. Hebel, S. Huber, B. Stanislawski, D. Hekmat, Stirred batch crystallization of a therapeutic antibody fragment, J. Biotechnol. 166 (2013) 206–211.
[112] H. Yang, W. Chen, P. Peczulis, J.Y.Y. Heng, Development and Workflow of a Continuous Protein Crystallization Process: A Case of Lysozyme, Cryst. Growth Des. 19 (2019) 983–991.
[113] M. Weselak, M.G. Patch, T.L. Selby, G. Knebel, R.C. Stevens, Robotics for Automated Crystal Formation and Analysis, Methods Enzymol. 368 (2003) 45–76.
[114] J.V. Parambil, M. Schaepertoens, D.R. Williams, J.Y.Y. Heng, Effects of oscillatory flow on the nucleation and crystallization of insulin, Cryst. Growth Des. 11 (2011) 4353–4359.
[115] J. Weaver, S.M. Husson, L. Murphy, S.R. Wickramasinghe, Anion exchange membrane adsorbers for flow-through polishing steps: Part II. Virus, host cell protein, DNA clearance, and antibody recovery, Biotechnol. Bioeng. 110 (2013) 500–510.
[116] N.E. Levy, K.N. Valente, K.H. Lee, A.M. Lenhoff, Host cell protein impurities in chromatographic polishing steps for monoclonal antibody purification, Biotechnol. Bioeng. 113 (2016) 1260–1272.
[117] M. Medrano, M.Á. Fuertes, A. Valbuena, P.J.P. Carrillo, A. Rodríguez-Huete, M. G. Mateu, Imaging and Quantitation of a Succession of Transient Intermediates Reveal the Reversible Self-Assembly Pathway of a Simple Icosahedral Virus Capsid, J. Am. Chem. Soc. 138 (2016) 15385–15396.
[118] F. Anouja, R. Wattiez, S. Mousset, P. Caillet-Fauquet, The cytotoxicity of the parvovirus minute virus of mice nonstructural protein NS1 is related to changes in the synthesis and phosphorylation of cell proteins, J. Virol. 71 (1997) 4671–4678.

[119] P. Cai, Q. Huang, D. Jiang, X. Rong, W. Liang, Microcalorimetric studies on the adsorption of DNA by soil colloidal particles, Colloids Surfaces B Biointerfaces. 49 (2006) 49–54.
[120] M. Vanderlaan, J. Zhu-Shimoni, S. Lin, F. Gunawan, T. Waerner, K.E. Van Cott, Experience with host cell protein impurities in biopharmaceuticals, Biotechnol. Prog. 34 (2018) 828–837.
[121] S. Chollangi, R. Parker, N. Singh, Y. Li, M. Borys, Z. Li, Development of robust antibody purification by optimizing protein-A chromatography in combination with precipitation methodologies, Biotechnol. Bioeng. 112 (2015) 2292–2304.
[122] X. Li, W. Chen, H. Yang, Z. Yang, J.Y.Y. Heng, Protein crystal occurrence domains in selective protein crystallisation for bio-separation, CrystEngComm. 22 (2020) 4566–4572.
[123] H. Yang, L. Huang, F. Zhang, V. Karde, Z. Yang, J.Y.Y. Heng, Gravity on Crystallization of Lysozyme: Slower or Faster? Cryst. Growth Des. 19 (2019) 7402–7410.
[124] B. Zhang, Y. Wang, S. Thi, V. Toong, P. Luo, S. Fan, L. Xu, Z. Yang, J.Y.Y. Heng, Enhancement of lysozyme crystallization using DNA as a polymeric additive, Crystals. 9 (2019) 186, https://doi.org/10.3390/cryst9040186.
[125] W. Chen, S.J. Park, F. Kong, X. Li, H. Yang, J.Y.Y. Heng, High Protein-Loading Silica Template for Heterogeneous Protein Crystallization, Cryst. Growth Des. 20 (2020) 866–873.
[126] B. Zhang, A.R. Mei, M.A. Isbell, D. Wang, Y. Wang, S.F. Tan, X.L. Teo, L. Xu, Z. Yang, J.Y.Y. Heng, DNA Origami as Seeds for Promoting Protein Crystallization, ACS Appl. Mater. Interfaces. 10 (2018) 44240–44246.
[127] U.V. Shah, N.H. Jahn, S. Huang, Z. Yang, D.R. Williams, J.Y.Y. Heng, Crystallisation via novel 3D nanotemplates as a tool for protein purification and bio-separation, J. Cryst. Growth. 469 (2017) 42–47.
[128] U.V. Shah, J.V. Parambil, D.R. Williams, S.J. Hinder, J.Y.Y. Heng, Preparation and characterisation of 3D nanotemplates for protein crystallisation, Powder Technol. 282 (2015) 10–18.
[129] D.S. Tsekova, D.R. Williams, J.Y.Y. Heng, Effect of surface chemistry of novel templates on crystallization of proteins, Chem. Eng. Sci. 77 (2012) 201–206.
[130] U.V. Shah, M.C. Allenby, D.R. Williams, J.Y.Y. Heng, Crystallization of proteins at ultralow supersaturations using novel three-dimensional nanotemplates, Cryst. Growth Des. 12 (2012) 1772–1777.
[131] U.V. Shah, D.R. Williams, J.Y.Y. Heng, Selective crystallization of proteins using engineered nanonucleants, Cryst. Growth Des. 12 (2012) 1362–1369.
[132] T. Delmas, M.M. Roberts, J.Y.Y. Heng, Nucleation and crystallization of lysozyme: Role of substrate surface chemistry and topography, J. Adhes. Sci. Technol. 25 (2011) 357–366.
[133] H. Yang, P. Peczulis, P. Inguva, X. Li, J.Y.Y. Heng, Continuous protein crystallisation platform and process: Case of lysozyme, Chem. Eng. Res. Des. 136 (2018) 529–535.
[134] M.M. Roberts, J.Y.Y. Heng, D.R. Williams, Protein crystallization by forced flow through glass capillaries: Enhanced lysozyme crystal growth, Cryst. Growth Des. 10 (2010) 1074–1083.
[135] A. McPherson, P. Shlichta, Heterogeneous and epitaxial nucleation of protein crystals on mineral surfaces, Science. 239 (1988) 385–387, https://doi.org/10.1126/science.239.4838.385.
[136] Y.W. Chen, C.H. Lee, Y.L. Wang, T.L. Li, H.C. Chang, Nanodiamonds as Nucleating Agents for Protein Crystallization, Langmuir. 33 (2017) 6521–6527.
[137] F. Hodzhaoglu, F. Kurniawan, V. Mirsky, C. Nanev, Gold nanoparticles induce protein crystallization, Cryst. Res. Technol. 43 (2008) 588–593.
[138] J.M. Kallio, N. Hakulinen, J.P. Kallio, M.H. Niemi, S. Kärkkäinen, J. Rouvinen, The contribution of polystyrene nanospheres towards the crystallization of proteins, PLoS One. 4 (2009), e4198.
[139] E. Saridakis, S. Khurshid, L. Govada, Q. Phan, D. Hawkins, G.V. Crichlow, E. Lolis, S.M. Reddy, N.E. Chayen, Protein crystallization facilitated by molecularly imprinted polymers, Proc. Natl. Acad. Sci. U. S. A. 108 (2011) 11081–11086.
[140] E. Curcio, E. Fontananova, G. Di Profio, E. Drioli, Influence of the Structural Properties of Poly(vinylidene fluoride) Membranes on the Heterogeneous Nucleation Rate of Protein Crystals, J. Phys. Chem. B. 110 (2006) 12438–12445.
[141] A.S. Thakur, G. Robin, G. Guncar, N.F.W. Saunders, J. Newman, J.L. Martin, B. Kobe, Improved success of sparse matrix protein crystallization screening with heterogeneous nucleating agents, PLoS One. 2 (2007), e1091.
[142] N.E. Chayen, E. Saridakis, R. El-Bahar, Y. Nemirovsky, Porous silicon: An effective nucleation-inducing material for protein crystallization, J. Mol. Biol. 312 (2001) 591–595.
[143] N.E. Chayen, E. Saridakis, R.P. Sear, Experiment and theory for heterogeneous nucleation of protein crystals in a porous medium, Proc. Natl. Acad. Sci. U. S. A. 103 (2006) 597–601.
[144] U.V. Shah, C. Amberg, Y. Diao, Z. Yang, J.Y.Y. Heng, Heterogeneous nucleants for crystallogenesis and bioseparation, Curr. Opin. Chem. Eng. 8 (2015) 69–75.
[145] P. Neugebauer, J.G. Khinast, Continuous crystallization of proteins in a tubular plug-flow crystallizer, Cryst. Growth Des. 15 (2015) 1089–1095.
[146] M. Pusey, W. Witherow, R. Naumann, Preliminary investigations into solutal flow about growing tetragonal lysozyme crystals, J. Cryst. Growth. 90 (1988) 105–111.
[147] X. Zhang, P. Zhang, K. Wei, Y. Wang, R. Ma, The study of continuous membrane crystallization on lysozyme, Desalination. 219 (2008) 101–117.
[148] L. Wang, G. He, X. Ruan, D. Zhang, W. Xiao, X. Li, X. Wu, X. Jiang, Tailored Robust Hydrogel Composite Membranes for Continuous Protein Crystallization with Ultrahigh Morphology Selectivity, ACS Appl. Mater. Interfaces. 10 (2018) 26653–26661.